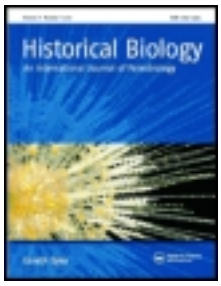

Historical Biology
Publication details, including instructions for authors and subscription information:
http://www.tandfonline.com/loi/ghbi20

Postcranial morphology and locomotion of the eocene raoellid *Indohyus* (Artiodactyla: Mammalia)

Lisa Noelle Cooper [a b], J. G.M. Thewissen [a], Sunil Bajpai [c] & B. N. Tiwari [d]

[a] Department of Anatomy and Neurobiology, Northeastern Ohio Medical University, 4209 State Route 44, Rootstown, OH, 44272, USA

[b] School of Biomedical Sciences, Kent State University, Kent, OH, 44242, USA

[c] Department of Earth Sciences, Indian Institute of Technology, Roorkee, Uttarakhand, 247 667, India

[d] Wadia Institute of Himalayan Geology, Dehra Dun, Uttarakhand, 248 001, India

Available online: 01 Nov 2011

To cite this article: Lisa Noelle Cooper, J. G.M. Thewissen, Sunil Bajpai & B. N. Tiwari (2011): Postcranial morphology and locomotion of the eocene raoellid *Indohyus* (Artiodactyla: Mammalia), Historical Biology, DOI:10.1080/08912963.2011.624184

To link to this article: http://dx.doi.org/10.1080/08912963.2011.624184

Historical Biology
iFirst article, 2011, 1–32

Postcranial morphology and locomotion of the eocene raoellid *Indohyus* (Artiodactyla: Mammalia)

Lisa Noelle Cooper[a,b]*, J.G.M. Thewissen[a1], Sunil Bajpai[c2] and B.N. Tiwari[d3]

[a]*Department of Anatomy and Neurobiology, Northeastern Ohio Medical University, 4209 State Route 44, Rootstown, OH 44272, USA;* [b]*School of Biomedical Sciences, Kent State University, Kent, OH 44242, USA;* [c]*Department of Earth Sciences, Indian Institute of Technology, Roorkee, Uttarakhand 247 667, India;* [d]*Wadia Institute of Himalayan Geology, Dehra Dun, Uttarakhand 248 001, India*

(*Received 26 July 2011; final version received 13 September 2011*)

Raoellids are small, raccoon-sized Eocene artiodactyls, closely related to archaic cetaceans (archaeocetes) that have poor representation of postcranial elements in the fossil record. Little is known of the aquatic and terrestrial locomotor affinities of raoellids due to the paucity of their fossil record, leaving a critical gap in our understanding of the earliest portion of the artiodactyl marine invasion. To address this gap, a comparative morphological analysis of the postcranial elements was undertaken based on newly recovered elements of the raoellid *Indohyus*, archaeocetes and extant artiodactyls. Greater than 200 postcranial elements of *Indohyus* were described, and some limb element cross-sections were visualised via paleohistological thin sections and CT scans. Results show that during terrestrial locomotion, *Indohyus* probably had a digitigrade posture and mediolaterally stabilised limbs that functioned mostly in flexion and extension within the parasagittal plane. Quantification of midshaft cross-sectional area for some elements of *Indohyus* showed an osteosclerotic cortex, a skeletal characteristic associated with aquatic behaviours. *Indohyus* may represent a critical intermediate in the evolution of the cetacean terrestrial-to-aquatic body plan, as it bears gracile postcranial element proportions similar to a terrestrial artiodactyl but also an incipient form of osteosclerosis compared to pakicetid archaeocetes.

Keywords: Cetacea; Artiodactyla; Raoellidae; *Indohyus*; postcrania; osteosclerosis

Abbreviations: *AMNH, American Museum of Natural History; CMNH, Cleveland Museum of Natural History; GSP-UM, Geological Survey of Pakistan-University of Michigan; H-GSP, Howard University-Geological Survey of Pakistan; HT, Collection of J.G.M. Thewissen; IITR, Indian Institute of Technology, Roorkee, India; IVAU, Instituut voor Aardwetenschappen, Utrecht, Netherlands; RR, A. Ranga Rao Collection of India currently housed at the Department of Anatomy and Neurobiology at the Northeastern Ohio Universities College of Medicine, Ohio; USGS, United States Geological Survey; USNM, Smithsonian Institution, United States National Museum of Natural History*

Introduction

Archaeocete and raoellid artiodactyls

Over the past 20 years, the land-to-sea transition of a single lineage of fossil artiodactlys, archaic cetaceans (archaeocetes), has been documented by several well-preserved fossils (Gingerich et al. 1994, 2001; Thewissen et al. 1994, 2001a, 2001b; Hulbert 1998; Hulbert et al. 1998; Bajpai and Thewissen 2000; Fordyce and de Muizon 2001; Geisler 2001; Uhen 2004; Gingerich et al. 2009; Thewissen and Bajpai 2009; Thewissen et al. 2009). These fossils show changes in the postcranial skeleton that facilitated an aquatic lifestyle, including spinal elongation, changes in vertebral configuration to support tail-based propulsion, hindlimb reduction and shifting of the forelimb from a weight-bearing hoofed limb to a lift-generating hydrofoil (e.g. Fish and Battle 1995; Thewissen and Fish 1997; Buchholtz 1998; Bajpai and Thewissen 2000; Gingerich et al. 2001; Madar et al. 2002; Gingerich 2003; Uhen 2004; Thewissen et al. 2006, 2009; Cooper et al. 2008; Thewissen and Bajpai 2009; Weber et al. 2009). Surprisingly, the earliest known fossil archaeocetes (pakicetids) already possessed a suite of well-developed skeletal morphologies indicative of a semi-aquatic lifestyle, including a modified vertebral column that allowed undulations of the tail and pelvic girdle for aquatic locomotion, and may have had webbed feet (Madar 2007). In addition, pakicetid long bones had extraordinarily thickened cortices, while the medullary cavities were tiny (Madar 2007; Thewissen et al. 2007). This skeletal morphology, termed osteosclerosis, is unlike the cross-sectional architecture displayed by terrestrial taxa, which have thinner bone cortices and larger, vacant medullary cavities. In pakicetids, the thickened cortex probably functioned as skeletal ballast to counteract body buoyancy during aquatic manoeuvres. Taken together, these skeletal morphologies suggest that pakicetids had a semi-aquatic lifestyle. This skeletal thickening therefore evolved in semi-aquatic archaeocetes

*Corresponding author. Email: l.noelle.cooper@gmail.com

ISSN 0891-2963 print/ISSN 1029-2381 online

http://dx.doi.org/10.1080/08912963.2011.624184
http://www.tandfonline.com

before the appearance of obligatorily aquatic cetaceans that were no longer able to support their weight on land (Gray et al. 2007; Madar 2007). Virtually nothing is known of the evolution of these skeletal morphologies between terrestrial artiodactyl taxa and semi-aquatic pakicetids. By describing the postcranial skeleton of *Indohyus* (Ranga Rao 1971), this study aims to further our understanding of the sequence of evolutionary events that lead to the successful acquisition of skeletal morphologies that supported aquatic habits of early cetaceans. Furthermore, a comparison of bone gross and cross-sectional morphologies between terrestrial artiodactyls, pakicetids and *Indohyus* was made to reconstruct how internal bone architecture changed during the land-to-sea transition.

Family Raoellidae

A central challenge in the study of cetacean origins is in identifying which fossil artiodactyl family was the closest relative of archaeocetes. Early molecular analyses found that cetaceans were most closely related to artiodactyls (even-toed ungulates, e.g. pigs, deer, *Hippopotamus*, camels, antelope, cows and sheep; Graur and Higgins 1994; Montgelard et al. 1997; Liu and Miyamoto 1999; Lum et al. 2000). Morphological support for this hypothesis was found in the ankle bones of archaic fossil cetaceans that closely resembled those of artiodactyls (Gingerich et al. 2001; Thewissen et al. 2001a, 2001b). Molecular analyses within Artiodactyla found that *Hippopotamus* (Linnaeus 1758) is the closest modern relative to cetaceans (e.g. Shedlock et al. 2000; Geisler and Uhen 2003; Boisserie et al. 2005b; Geisler and Uhen 2005; Price et al. 2005; Geisler et al. 2007; Marcot 2007; Geisler and Theodor 2009). Unfortunately, fossil evidence of this close relationship is lacking as a 30-million year gap exists between the appearance of the first archaeocetes and the first hippopotamids. The earliest fossil hippopotamid, *Kenyapotamus* (Pickford 1983), was recovered from middle Miocene deposits in Kenya dating from 14 to 16 Ma (Pickford 1983; Behrensmeyer et al. 2002; Boisserie et al. 2005a, 2005b), while the earliest archaeocetes were recovered from early Eocene sediments over 50 Ma (Bajpai and Gingerich 1998). More recently, phylogenetic hypotheses of the fossil sister taxon of cetaceans ranged from the entire artiodactyl order (Thewissen et al. 2001b), cebochoerids (Theodor and Foss 2005), an anthracotheroid clade (Boisserie et al. 2005b), mesonychids (O'Leary 1998; O'Leary and Gatesy 2008) or possibly to the artiodactyl family Raoellidae that was known only from fragmentary dental material (Geisler and Uhen 2003, 2005; Geisler et al. 2007). Further evidence of a close raoellid–archaeocete relationship was provided by Thewissen et al. (2007) based on the most complete collection of cranial and postcranial raoellid material to date. In a morphological phylogenetic analysis, Thewissen et al. (2007) found that the raoellid *Indohyus* was sister to archaeocetes, and therefore all cetaceans. Synapomorphies with cetaceans, and not other artiodactyls, include the presence of an involucrum, anteroposterior arrangement of incisors in the jaw, and high crowns in the posterior premolars (Thewissen et al. 2007). Furthermore, based on the analyses of limb bone thickness and dental isotopic data, Thewissen et al. (2007) hypothesised that *Indohyus* most likely occupied a freshwater habitat (see reviews in Thewissen et al. 2009; Cooper and Thewissen 2010). Additional support for a raoellid–archaeocete sister relationship came from a recent combined molecular and morphological phylogenetic analyses of Artiodactyla (Geisler and Theodor 2009). Based on a separate parsimony analysis of a combined morphological and molecular data set (Spaulding et al. 2009), *Indohyus* fell out as closely related to cetaceans, but the phylogenetic position of *Indohyus* was unstable depending on the choice of taxa and character sets. Taken together, the most consistent interpretation of these phylogenetic analyses (Geisler and Uhen 2003, 2005; Geisler et al. 2007; Thewissen et al. 2007; Geisler and Theodor 2009; Spaulding et al. 2009) is that Raoellidae (most specifically *Indohyus*) is the closest relative to archaeocetes and all cetaceans, while *Hippopotamus* is the closest extant relative.

Raoellid fossils (Sahni et al. 1981) have primarily been recovered from middle Eocene sediments in Pakistan and India (Russell and Zhai 1987; Thewissen et al. 2001a). Most of the early reports were limited to the dental material (Pilgrim 1940; Dehm and zu Oettingen-Spielberg 1958; Ranga Rao 1971; Sahni and Khare 1971; Gingerich 1977; West 1980; Ranga Rao and Misra 1981; Sahni et al. 1981; Kumar and Sahni 1985; Thewissen et al. 1987, 2001a) and represented several genera, including *Indohyus* (Ranga Rao 1971), *Khirtharia* (Pilgrim 1940), *Kunmunella* (Sahni and Khare 1971) and *Metkatius* (Kumar and Sahni 1985). These taxa were divided into two broad morphological categories: bunodont forms (e.g. *Khirtharia* and *Metkatius*) and more lophodont forms (e.g. *Kunmunella* and *Indohyus*) (Theodor et al. 2007). *Indohyus* (Ranga Rao 1971; Sahni and Khare 1971) is represented by two taxa, *Indohyus indirae* (Ranga Rao 1971) and I. major. *Indohyus* major is roughly twice the size of *I. indirae* (Thewissen et al. 1987). The first mostly complete skull and postcranial elements of *Indohyus* were prepared from an assemblage of disarticulated remains collected by the Indian geologist A. Ranga Rao in a middle Eocene bone bed at Sindkhatudi in the Kalakot region of the state of Jammu & Kashmir on the Indian side of the Line of Control (Thewissen et al. 2007). A limited number of bones have been described, and species-level taxonomy has yet to be worked out. Further preparation has unearthed over 300 disarticulated bones (cranial and postcranial) pertaining to a minimum of at least 25 individuals (based on cranial and dental elements), allowing further analyses.

Several more-or-less lophodont raoellids have been described from Kalakot: *I. indirae*, *I. kalakotensis*, *Raoella*

dograi, *Kunmunella rajauriensis*, *K. transversa* and *Metkatius kashmiriensis*, and all but the last of these were synonymised by Russell and Zhai (1987) with *I. indirae* (Sahni and Khare 1971; Thewissen et al. 2001a; Theodor et al. 2007). The specimens described by Thewissen et al. (2007) and in this study were assigned to the genus *Indohyus* based on multiple well-preserved skulls and lower jaws. Dental evidence showed that more than 90% of the specimens recovered at Sindkhatudi were raoellids, and associated postcranial elements shared a similar body size. Other taxa from Kalakot have a similar body size (e.g. tapiroids), but the morphology of postcranial elements is unlike those discussed here. It could be that the assignment to the genus *Indohyus* may be revised, as some elements may be those of *Metkatius*; however, these genera are currently synonymised (Russell and Zhai 1987). The specimens could also belong to the genus *Khirtharia*, a bunodont form; however, undescribed limited skeletal remains are known from the collection described by Pilgrim (1940) and this genus is very rare at Sindkhatudi. With increasing collections of dental material, several raoellids may be distinguished, but, at present and for our purpose, the most conservative interpretation is to consider all described postcranial elements as belonging to *Indohyus*.

This study compared the gross morphology of the postcranial skeleton of *Indohyus* with that of terrestrial artiodactyl lineages and archaeocetes. This study aims to first reconstruct the locomotor capabilities of *Indohyus* both in out of the water, and second to document the sequences of morphological events that took place during the incipient phases of the land-to-sea invasion by cetaceans. *Indohyus* was compared to the representatives of the earliest fossil artiodactyls (diacodexids) as they are thought to occupy a terrestrial niche. The diacodexid *Diacodexis* was recovered from early Eocene sediments (Theodor et al. 2007) of North America (Krishtalka and Stucky 1985; Rose 1985; Krishtalka and Stucky 1986; Gingerich 1989; Gunnell and Bartels 2001), Europe (Sudre et al. 1983) and Asia (Thewissen et al. 1983; Thewissen and Hussain 1990; Bajpai et al. 2005). Those specimens of *Diacodexis pakistanensis* recovered from Asia were renamed *Gujaratia pakistanensis* (Thewissen et al. 1983; Thewissen and Hussain 1990; Bajpai et al. 2005; Theodor et al. 2007). This study compared the skeletal elements of *Indohyus* with diacodexid elements recovered from North America (i.e. Rose 1985) and Asia (Thewissen et al. 1983). Besides terrestrial diacodexids, *Indohyus* postcranial elements were also compared to those of the earliest fossil family of archaeocetes (pakicetids, Madar 2007). Skeletal and isotopic analyses of pakicetid cetaceans recovered from middle Eocene sediments in Pakistan (e.g. West 1980; Gingerich and Russell 1981, 1990; Thewissen and Hussain 1998; Thewissen et al. 2001b; Madar 2007) showed that pakicetids occupied a semi-aquatic niche (Thewissen et al. 1996; Roe et al. 1998; Clementz et al. 2006; Gray et al. 2007; Madar 2007). *Indohyus* was also compared to a modern ruminant, the terrestrial tragulid artiodactyl *Tragulus javanicus* (lesser mouse deer, Brisson 1762). *Tragulus* was chosen for comparison as it is one of the smallest modern artiodactyls (Endo et al. 2006), and is approximately of the same body size as that of *Indohyus*. *Tragulus* is endemic to southern Asia and inhabits heavy lowland forests near shallow bodies of water (Nowak 1991) and is known to stay submerged for extended periods of time (from five to 60 min) to escape predation (Meijaard et al. 2010).

To reconstruct the evolution of the skeleton along the cetacean land-to-sea transition, this study also compared the cross-sectional geometries of long-bone midshafts of *Indohyus* with fossil and modern artiodactyls and fossil cetaceans. Terrestrial vertebrates are known to have thinner bone cortices and large medullary cavities compared to most amphibious and semi-aquatic taxa (e.g. Wall 1983; Fish and Stein 1991; Gray et al. 2007; Madar 2007; Thewissen et al. 2007; Kriloff et al. 2008). Thewissen et al. (2007) showed that the long-bone cortices of *Indohyus* were slightly thickened compared to some terrestrial artiodactyls, but were much thinner than those of pakicetid archaeocetes. Specifically, Thewissen et al. (2007) noted that the femur of *Indohyus* displayed a thickened cortex, but this comparison was only made with a small sample of artiodactyl taxa. This study furthers the analysis of long-bone cross-sectional evolution by adding three additional modern taxa (*Hyemoschus* (Ogilby 1841), *Tragulus* and *Capra* (Linnaeus 1758)) and by expanding the quantitative analysis to include the tibia, ulna, metapodials, ribs and a vertebra.

Materials and methods

Postcranial elements of the raoellid *Indohyus* described here are part of the A. Ranga Rao (RR) fossil collection (see Appendix) and were prepared and curated by one of us (J.G.M.T.).

Anatomical comparisons were made with fossil diacodexid artiodactyls including published material and casts of *G. pakistanensis* (originally described as *Diacodexis*, Thewissen et al. 1983) and *Diacodexis metsiacus* (Rose 1985). Comparisons were also made with the elements of pakicetids (Thewissen et al. 2001a, 2001b; Madar 2007) and an ambulocetid archaeocete (*Ambulocetus natans* H-GSP 18507 (Thewissen et al. 1996; Madar et al. 2002)) was recovered by the Howard Geological Survey of Pakistan. Comparisons with extant artiodactyls were mostly made with *T. javanicus* (CMNH 17917, 21826), as it is roughly equivalent in body size to *Indohyus*. Locomotor comparisons were also made with the extant cursorial artiodactyls *Odocoileus virginianus*

Zimmerman, 1780 (CMNH 2026, 21888) and *O. hemionus* Rafinesque, 1817 (CMNH 4980).

This study compared the postcranial element cross-sectional geometries of *Indohyus*, artiodactyls and cetaceans, via three visualisation methods: examination of the midshaft of broken bones, paleohistological sections of long-bone midshafts and high resolution CT scans through the midshaft of long bones and centres of vertebrae. Cross-sections were visualised in a total of 44 elements, and diameter measurements were calculated along the anteroposterior and mediolateral planes. Cortical thickness is known to vary along the proximo-distal length of a given element, and visualisation and quantification of midshaft dimensions have been shown to be a reliable indicator of different ecological habitats occupied by vertebrates (e.g. Kriloff et al. 2008). This study utilised high resolution CT scans for most of the bones with small midshaft diameters, taken on a XCT540 Research M scanner located at the Northeastern Ohio Medical University and a medical scanner at the Akron City Hospital in Ohio. This study also employed paleohistological thin sections of the midshafts of long bone of *Indohyus* (femur (RR 42), humerus (RR 157)) and the pakicetid *Ichthyolestes pinfoldi* (H-GSP 96227) (Thewissen et al. 2007). For each bone cross-section, cortical bone thickness was expressed as the ratio of whole bone diameter to medullary cavity diameter.

Results

Ribs

Ribs of *Indohyus* (RR 168, 217, 221, 222, 235, 243, 244, 245, 305; Figure 1.1–1.2) and *Tragulus* (CMNH 17917, 21826) are gracile compared to the greatly thickened (pachyostotic) ribs of pakicetids (e.g. H-GSP 92060, 96436, 30131).

Cervical vertebrae

Atlas

The atlas of *Indohyus* (RR 165; Figure 1.3–1.4) has a left transverse process that extends caudally compared to the right, unlike those of pakicetids and *Tragulus*. Both transverse processes are thin in *Indohyus* and *Tragulus*, while in pakicetids (H-GSP 96021, 96566) these processes are comparatively robust. Ventral surfaces of the transverse processes are deeply excavated in *Indohyus*, pakicetids and *Tragulus*, but shallowly concave in *Diacodexis* (Rose 1985). The dorsal arch of the atlas is longer craniocaudally than the ventral arch in *Indohyus* (RR 86) and pakicetids (the ventral arches of H-GSP 96021 and 96566 were originally interpreted as the dorsal arches by Madar (2007)). The apex of the dorsal arch in the atlas of *Indohyus* and pakicetids bears a slightly raised, conical projection along its cranial surface, while this structure is a transverse ridge in *Tragulus*. The cranial facets for articulation with the occipital condyles of the atlas of *Indohyus* form a wide and deep socket surrounding the vertebral canal, with facets extending along the lateral surfaces of the canal. Around the vertebral canal a pair of distinct dorsolateral and ventrolateral articular facets is present in *Tragulus*, while these facets are combined in the atlas of *Indohyus* and pakicetids. The caudal facets of the atlas, which articulate with the axis, are shallow and slightly concave in *Diacodexis* (Rose 1985), *Indohyus* and pakicetids, but gently convex in *Tragulus*. Dimensions of the atlas (RR 165) are as follows: mediolateral width is 42.0 mm; dorsoventral height is 10.7 mm; cranial view neural canal width is 8.7 mm and cranial view neural canal height is 2.8 mm.

Cervical vertebra 3

Cervical vertebra 3 (Ce3) of *Indohyus* (RR 33) is tentatively identified based on the relative size of the body and articular facets. Its dorsal arch is long craniocaudally and bears a longitudinal crest that gives rise to a low spinous process, as in *Tragulus* (CMNH 21826). The Ce3 cranial facets of *Indohyus* extend from the dorsal arch, are directed ventrally, slightly convex and elliptical in shape. These facets are much larger in *Indohyus* than in *Tragulus*. The body is wide and short.

Cervical vertebra 4

Cervical vertebra 4 (Ce4) of *Indohyus* (RR 342; Figure 1.5) is tentatively identified. It is smaller in all dimensions compared to Ce5 and Ce6, but bears larger articular facets than Ce3. Ce4 of *Tragulus* (CMNH 21826) bears long and narrow cranial facets, but these facets are tiny and rounded in *Indohyus*. Ce4 caudal facets of *Indohyus* and *Tragulus* are similar in shape and orientation. Laminae of the dorsal arch of *Indohyus* form a neural canal with a triangular cross-section, and a narrow surface area for the attachment of epaxial musculature, which is in strong contrast to the flattened laminae of *Tragulus*. The vertebral body is opisthocoelous. The scalene processes of *Indohyus* Ce4 are damaged, obscuring their full extent. Dimensions of Ce4 (RR 342) are as follows: craniocaudal length is 9.3 mm, mediolateral width is 27.9 mm, dorsoventral height is 25.1 mm, cranial view neural canal mediolateral width is 7.5 mm and cranial view neural canal dorsoventral height is 7.4 mm.

Cervical vertebra 5

Cervical vertebra 5 (Ce5) of *Indohyus* (RR 38, Figure 1.9–1.10; RR 136 Figure 1.6–1.8; RR 332, 337) is identified based on the orientation and length of the transverse processes, and size of the vertebral body. This

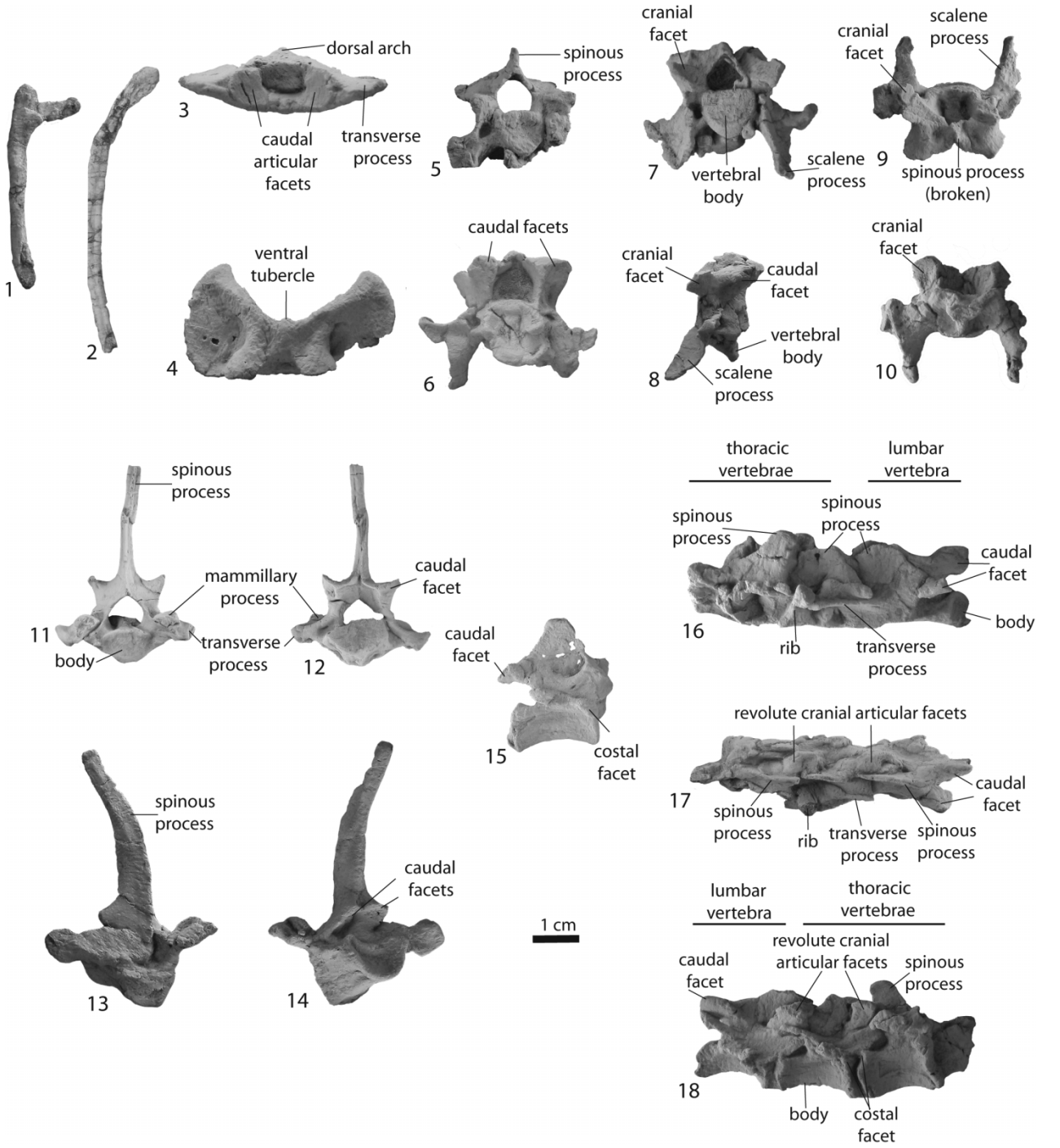

Figure 1. Ribs and vertebrae of *Indohyus* (Ranga Rao 1971). 1, anterior rib (RR 243); 2, posterior rib (RR 244); 3, 4, atlas (RR 165) in caudal and ventral views; 5, cervical vertebra 4 (RR 342) in caudal view; 6, 7, 8, cervical vertebra 5 (RR 136) in caudal, cranial and lateral views; 9, 10, cervical vertebra 5 (RR 38) in dorsal and ventral views; 11, 12, cranial thoracic vertebra (RR 247) in cranial and caudal views; 13, middle thoracic vertebra (RR 85) in cranial and caudal views; 15, caudal thoracic vertebra (RR 25) in lateral view; 16, 17, 18, two articulated terminal thoracic vertebrae in articulation with the cranial-most lumbar vertebra (RR 239), showing shift in angle of inclination of spinous processes in left lateral, dorsal and right lateral views. Scale bar is 1 cm in length.

vertebra has delicate processes, as in *Tragulus*, and is gracile compared to the robust body and processes of the Ce5 of pakicetids (H-GSP 92082). In *Indohyus*, the steep laminae of the dorsal arch create a triangular neural canal (RR 136, 332, 337). The cranial facets are dorsal-facing, flat and circular in shape in *Indohyus*, while those of *Tragulus* are near rectangular and gently convex. In most artiodactyls, the cranial facets are convex. Caudal facets

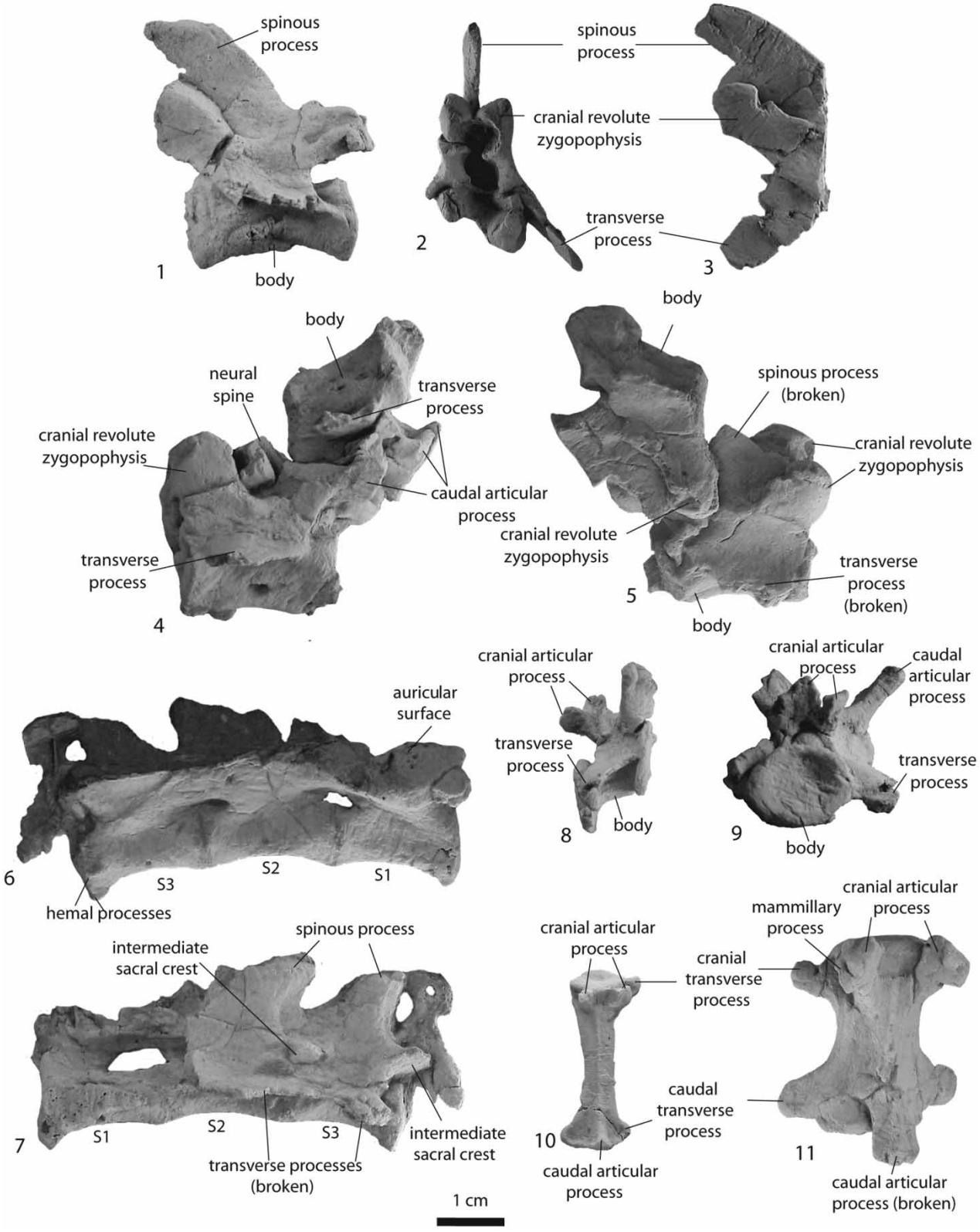

Figure 2. Vertebrae of *Indohyus* (Ranga Rao 1971). 1, lumbar vertebra (RR 343) in lateral view; 2, 3, lumbar vertebra (RR 215) in cranial and caudal views; 4, 5, two attached lumbar vertebrae (RR 296) with the bottom vertebra in left lateral view and right lateral views; 6, 7, sacrum (RR 156) in right lateral and left lateral views; 8, 9, Caudal vertebra (RR 339) in lateral and cranial views; 10, terminal caudal vertebra (RR 249) in dorsal view; 11, caudal vertebra (RR 294) in dorsal view. Scale bar is 1 cm in length.

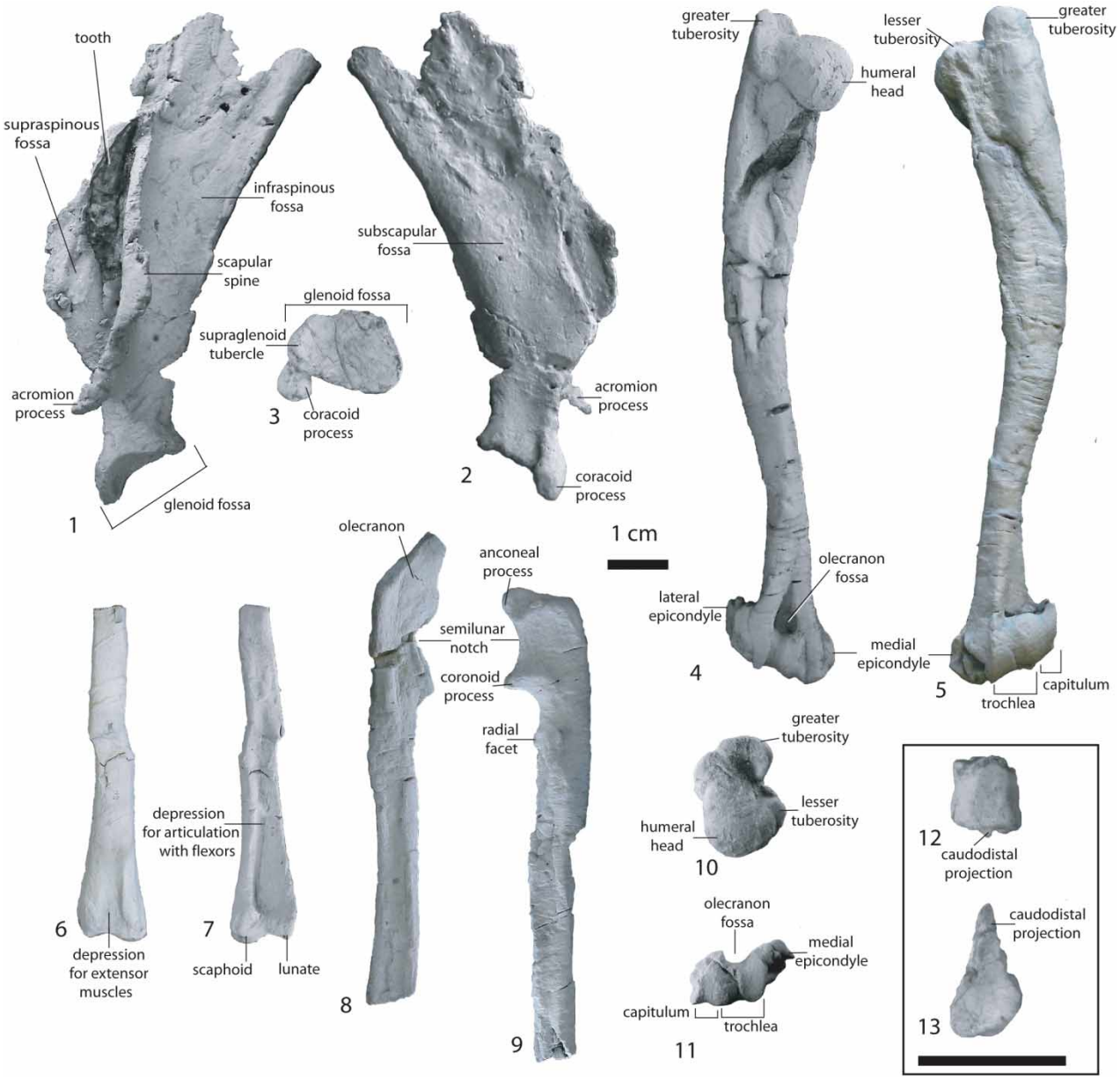

Figure 3. Forelimb elements of *Indohyus* (Ranga Rao 1971). 1, 2, left scapula (RR 155) in lateral and medial views; 3, glenoid of the scapula (RR 263) in ventral view; 4, 5, 10, 11, left humerus (RR 149) in caudal, cranial, proximal and distal views; 6, 7, radius (RR 265) in cranial and caudal views; 8, left ulna (RR 39) in medial view; 9, right ulna (RR 149) in medial view; 12, 13, magnum (RR 250) in cranial and distal views. Scale bars are 1 cm in length.

of *Indohyus* are ventral–lateral facing, circular and slightly concave, while those of *Tragulus* are triangular. The cranial surface of the vertebral body is triangular, while the caudal surface is circular in *Indohyus* (RR 136) and *Tragulus*, but the cranial surface is circular in pakicetids (H-GSP 92082). The transverse process of Ce5 of *Indohyus* bears two projections: a small laterally directed projection, and a long cranially directed projection the scalene processes. The scalene processes of *Indohyus* are much larger than those of *Tragulus*. The body is wide and short. Dimensions of Ce5 (RR 136) are as follows: craniocaudal length is 16.8 mm, mediolateral width is 35.8 mm, dorsoventral height is 30.0 mm, cranial view neural canal mediolateral width is 6.9 mm and cranial view neural canal dorsoventral height is 7.0 mm. Dimensions of Ce5 (RR 38) are as follows: craniocaudal length is 27.9 mm, mediolateral width is 31.0 mm, dorsoventral height is 12.8 mm, cranial view neural canal mediolateral width is 6.9 mm and cranial view neural canal dorsoventral height is 4.0 mm.

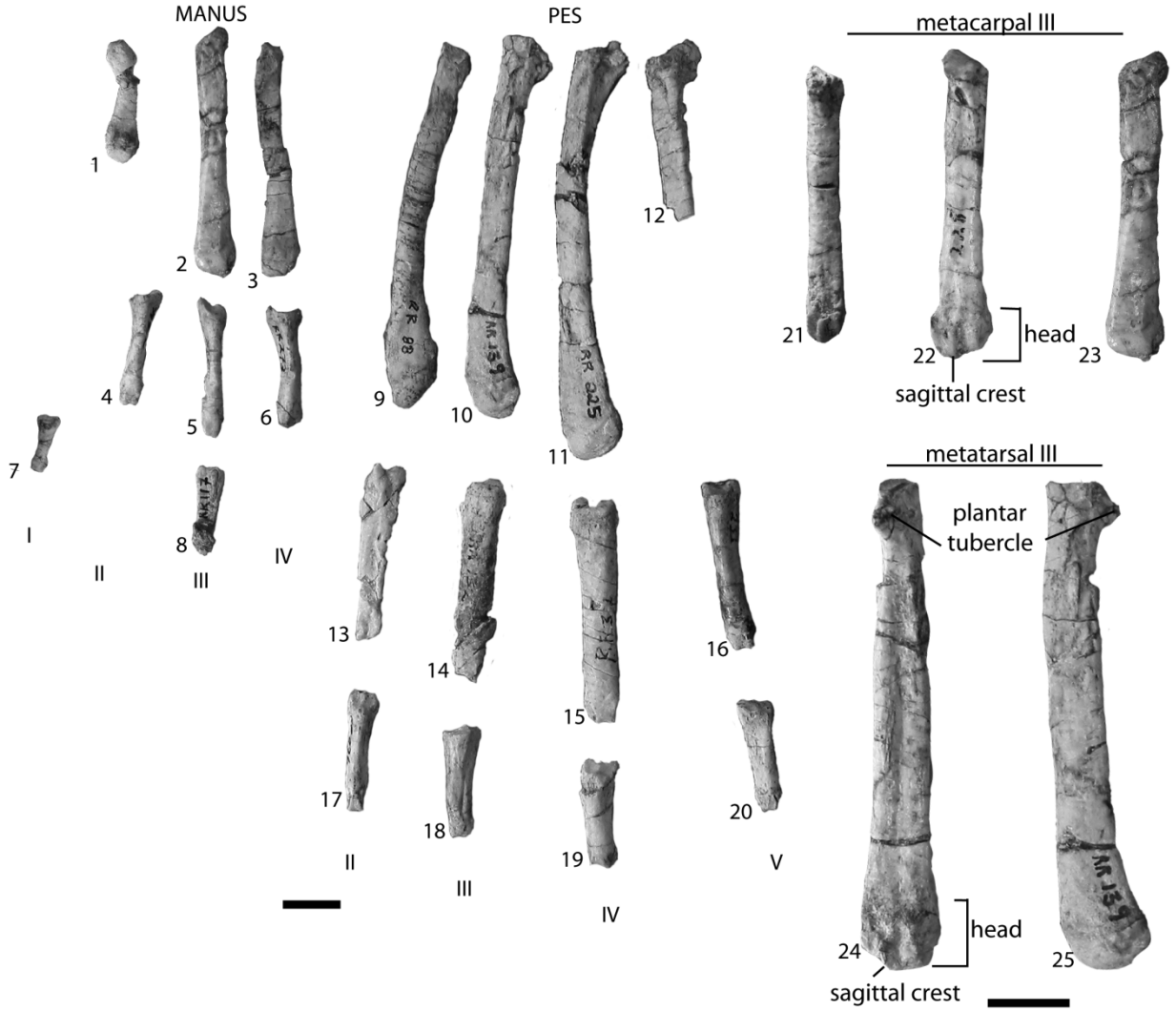

Figure 4. The manus and pes of *Indohyus* (Ranga Rao 1971). 1, metacarpal I (RR 297); 2, left metacarpal III (RR 228); 3, metacarpal IV (RR 270); 4, proximal manual phalanx (RR 274); 5, proximal manual phalanx (RR 273); 6, proximal manual phalanx (RR 201); 7, intermediate manual phalanx I (RR 234); 8, intermediate manual phalanx (RR 117); 9, peripheral metatarsal (RR 88); 10, right metatarsal III (RR 139); 11, left metatarsal IV (RR 225); 12, peripheral metatarsal (RR 47); 13, proximal pedal phalanx (RR 200); 14, proximal pedal phalanx (RR 132); 15, proximal pedal phalanx (RR 37); 16, proximal pedal phalanx (RR 231); 17, intermediate pedal phalanx (RR 276); 18, intermediate pedal phalanx (RR 277); 19, intermediate pedal phalanx (RR 125); 20, intermediate pedal phalanx (RR 230); 21, enlarged view of left metacarpal III (RR 271) in plantar view; 22, 23, left metacarpal III (RR 228) in plantar and dorsal views; 24, 25, right metatarsal III (RR 139) in plantar and dorsal views. Roman numerals indicate digit identity. Scale bars are 1 cm in length.

Cervical vertebra 7

Cervical vertebra 7 of *Indohyus* (Ce7; RR 195) is identified based on the absence of a transverse foramen and a body with a tiny cranial surface and large caudal surface. The spinous process projects vertically and is flanked by a pair of caudal facets in both *Indohyus* and *Tragulus*. These caudal facets are directed caudally in *Indohyus*, but directed caudomedially in *Tragulus*. In *Indohyus*, laminae form a steep triangular roof to the vertebral canal while its base is horizontal. Transverse processes project from the lateral part of the base of the lamina in *Indohyus*. The cranial surface of the vertebral body is half the width of the caudal surface in *Indohyus* and *Tragulus*. The body is wide and short. Dimensions of Ce7 (RR 195) are as follows: craniocaudal length is 8.6 mm, mediolateral width is 24.5 mm, dorsoventral height is 26.6 mm, cranial view neural canal mediolateral width is 10.3 mm and cranial view neural canal dorsoventral height is 6.0 mm.

Thoracic vertebrae

Cranial thoracic vertebrae

The thoracic vertebrae located in the cranial portion of the thoracic column (i.e. RR 20, 21, 247, Figure 1.11 – 1.12) of

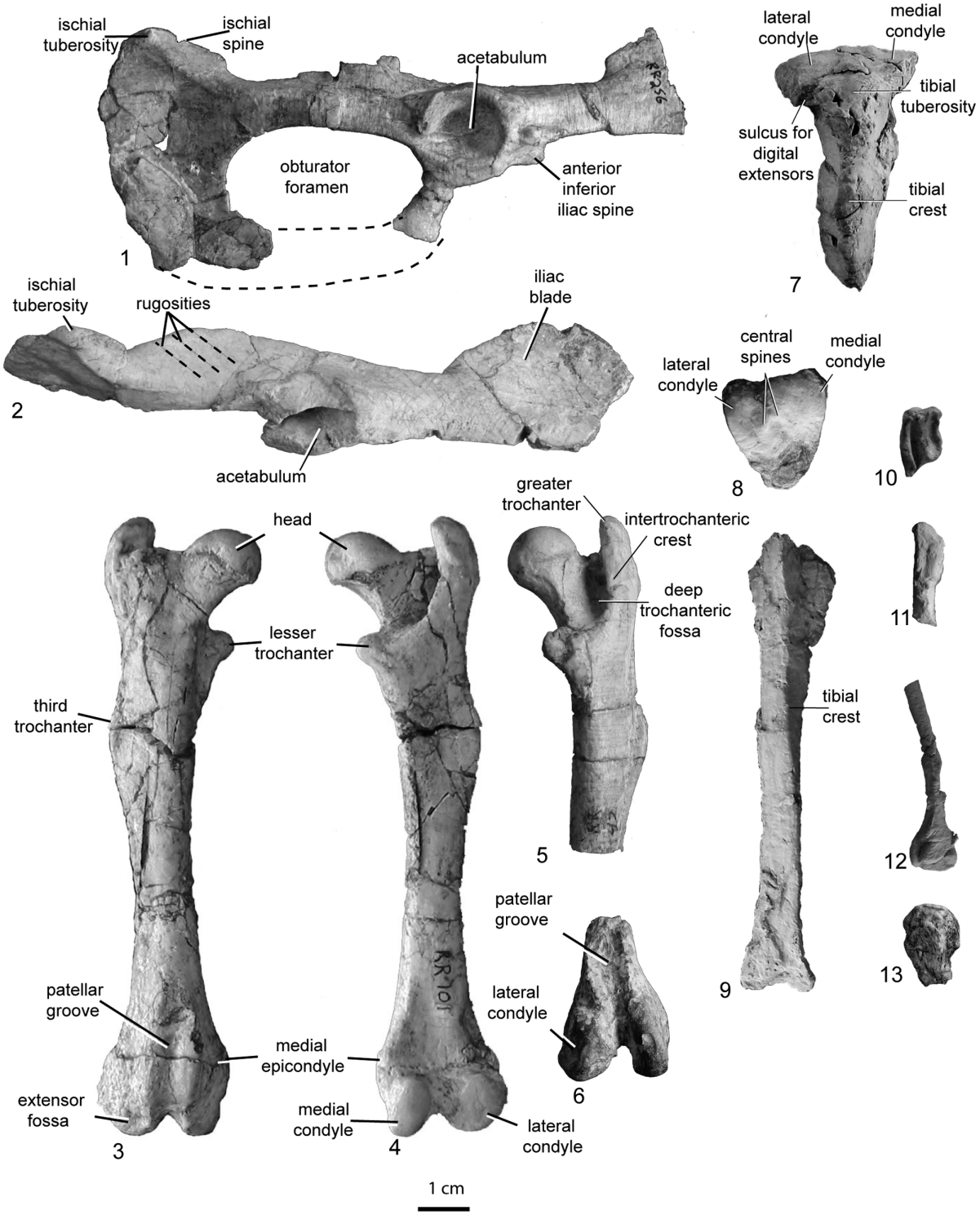

Figure 5. Pelvic limb elements of *Indohyus* (Ranga Rao 1971). 1, right innominate (RR 256) in lateral view; 2, right innominate (RR 257) in dorsal view; 3, 4, right femur (RR 101) in cranial and caudal views; 5, right femur (RR 42) in caudal view; 6, right femur (RR 133) in cranial view; 7, proximal fragment of right tibia (RR 84) in cranial view; 8, right tibial plateau (RR 22) in proximal view; 9, juvenile tibial shaft (RR 143) in cranial view; 10, tibia (RR 301), distal view; 11, proximal part of the fibula (RR 96); 12, distal part of the fibula (RR 295) in lateral view; 13, patella (RR 269) in cranial view. Scale bar is 1 cm in length.

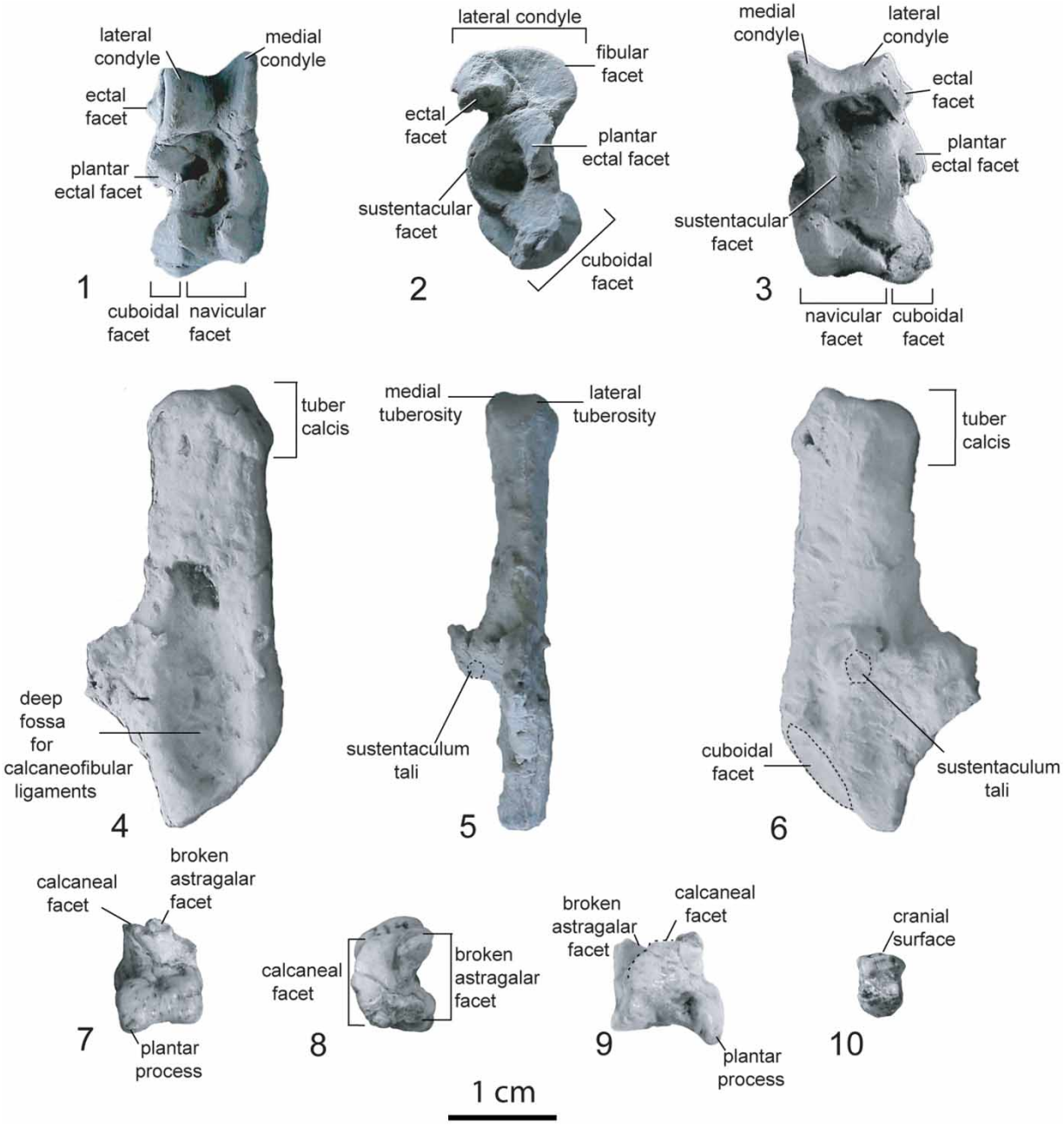

Figure 6. Tarsal elements of *Indohyus* (Ranga Rao 1971). 1, 2, 3, right astragalus (RR 224) in cranial, lateral and caudal views; 4, 5, 6, left calcaneus (RR 170) in lateral, cranial and medial views; 7, 8, 9, left cuboid (RR 214) in caudal, proximal, and lateral views; 10, ectomesocuneiform (RR 192) in distal view. Scale bar is 1 cm in length.

Indohyus and *Tragulus* (CMNH 21826) display slender spinous processes, whereas the spinous processes of pakicetids (H-GSP 96516) are relatively tall and robust. In *Indohyus* (RR 247) and pakicetids (H-GSP 96248), caudal articular surfaces located at the base of the spinous processes face caudolaterally, while in *Tragulus* they are ventral-facing. Left and right laminae articulate at a sharp angle in *Indohyus* and pakicetids (H-GSP 96248), creating a vertebral canal that is triangular in cross-section, while in *Tragulus*, these laminae maintain a gentle curvature and create a vertebral canal that is elliptical in cross-section. The centrum is wider mediolaterally as well as longer on the craniocaudal axis (RR 247). Mammillary processes (metapophyses) along the superior root of the transverse processes project cranially in *Indohyus* and *Tragulus*. The tips of the transverse processes in *Indohyus* (RR 247) have hemispherical, arcuate, lateral-facing costal foveae,

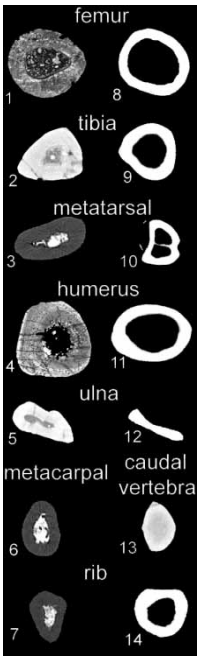

Figure 7. Bone cross-sectional geometries in *Indohyus* (Ranga Rao 1971) compared to terrestrial artiodactyls with an equivalent body size (*Tragulus* and *Hyemoschus*). 1, midshaft paleohistological section of femur of *Indohyus* (RR 42); 4, midshaft paleohistological section of the humerus (RR 157) of *Indohyus*; 2, midshaft CT scan of a tibia of *Indohyus* (RR 46); 3, midshaft CT scan of a metatarsal of *Indohyus* (RR 225); 5, midshaft CT scan of an ulna (RR 39) of *Indohyus*; 6, midshaft CT scan of a metacarpal (RR 228) of *Indohyus*; 7, midshaft CT scan of a rib (RR 217) of *Indohyus*; 13, midshaft CT scan of a caudal vertebra (RR 249) of *Indohyus*; 8, midshaft CT scan of the femur of *Tragulus* (CMNH 17917); 9, midshaft CT scan of the tibia of *Tragulus* (CMNH 17917); 10, midshaft CT scan of the fused metatarsals (cannon bone) of *Tragulus* (CMNH 17917); 11, midshaft CT scan of the humerus of *Tragulus* (CMNH 17917); 12, midshaft CT scan of the ulna of *Tragulus* (CMNH 17917); 14, midshaft CT scan of the rib of *Hyemoschus* (CMNH 17918).

with a prominent rim encircling their cranial, caudal and dorsal surfaces (RR 247). In *Tragulus*, these foveae assume the shape of a cranial-facing arc. In *Diacodexis*, these foveae are directed vertically and laterally, ovate and convex (Rose 1985). Costal foveae along the cranial portion of the thoracic vertebrae are small, circular and directed ventrally in *Indohyus*, but are directed cranially in pakicetids (H-GSP 96410, 96248) and directed craniolaterally in *Tragulus*. Vertebral bodies of *Indohyus* are elliptical while those of *Tragulus* are heart-shaped and those of pakicetids are triangular (H-GSP 96248, 96410). Dimensions of one cranial thoracic vertebra (RR 247) are as follows: craniocaudal length is 9.2 mm, mediolateral width is 29.7 mm, dorsoventral height is 42.9 mm, cranial view neural canal mediolateral width is 7.4 mm and cranial view neural canal dorsoventral height is 7.0 mm.

Middle thoracic vertebrae

Compared to cranial thoracic vertebrae, the middle thoracic vertebrae (RR 85, 137, 242, 292) of *Indohyus* display a relatively tall spinous process (RR 85, Figure 1.13–1.14). These processes in *Indohyus* are still comparatively shorter than those of pakicetids (H-GSP 96516). The centrum is roughly equivalent in width and craniocaudal length in *Indohyus*, but is short in dorsoventral height, as in pakicetids (H-GSP 96516). The centra of middle thoracic vertebrae of *Indohyus* are relatively shorter than those of *Tragulus* while the spinous processes are similar in height. Middle thoracic vertebrae have a ventral keel (RR 137, 247), shaped like those of *Diacodexis* and pakicetids, but unlike the smooth arc-shaped ventral surfaces in *Tragulus*.

Caudal thoracic vertebrae

The thoracic vertebrae of *Indohyus* in the caudal portion of the thoracic column (i.e., RR 25, Figure 1.15; two of the three vertebra in RR 239, Figure 1.16–1.18; RR 344) display short and triangular spinous processes that are angled caudally in the penultimate thoracic vertebra, as in *Tragulus* and pakicetids. Flanking the spinous processes of *Indohyus* and *Tragulus* are cylindrical caudal articular surfaces that articulate with the revolute zygapophyses of adjacent vertebrae. Cranial articular surfaces (zygapophyses) are dorsoventrally thick and their dorsal lip locks the caudal articular surface of an adjacent vertebra in place. The vertebral bodies of *Indohyus* and *Tragulus* are craniocaudally long compared to cranial thoracic vertebrae. Dimensions of a caudal thoracic vertebra (RR 25) are as follows: craniocaudal length is 24.5 mm, mediolateral width is 8.0 mm and dorsoventral height is 28.2 mm.

Lumbar vertebrae

Lumbar vertebrae (RR 239, Figure 1.16–1.18; RR 343, Figure 2.1; RR 215, Figure 2.2–2.3; RR 296, Figure 2.4–2.5) of *Indohyus*, *Tragulus* and pakicetids (H-GSP 98154) display thin spinous processes, a craniocaudally long body and cylindrical and laterocaudally directed caudal facets. The lumbar spinous processes of pakicetids are relatively robust (H-GSP 98154, 98198). The cranial facets (zygapophyses) of *Indohyus* and *Tragulus* are revolute such that they cover the entire dorsal and lateral surface of an articulating caudal facet. In pakicetids, these zygapophyses are only partially revolute and display a dorsomedially directed facet (H-GSP 98198, 98154). A tiny, cylindrical transverse process extends craniolaterally from the body of a single specimen of *Indohyus* (RR 239, Figure 1.16–1.18), but in other cranial lumbar vertebrae (RR 296), the preserved bases of the transverse processes are directed cranioventrally, as in *Tragulus* and pakicetids

(H-GSP 98198, 98154). The cranial lumbar vertebrae of *Indohyus* display a craniocaudally long body, with relatively short spinous processes (RR 239), while more caudal lumbar vertebrae display dorsoventrally tall spinous processes, and longer transverse processes (RR 343, Figure 2.1; RR 215, Figure 2.2–2.3).

Sacral vertebra

The sacral vertebrae of *Indohyus* (RR 156, Figure 2.6–2.7) and pakicetids (H-GSP 30251) have spinous processes that are fused at the base of each process, while in *Tragulus* they are fused along their entire dorsoventral height. A total of three sacral vertebrae are present in *Indohyus*. S3 bears a pair of hemal processes along its ventral and caudal surface, as in S4 of pakicetids, but unlike the ventral processes of *Tragulus* that lack hemal processes. S2 and S3 display small, ovoid, caudolaterally directed facets that make up the intermediate sacral crest. These processes are long, cylindrical and directed caudally in pakicetids, while they are fused into a single longitudinal crest in all vertebrae but S4 in *Tragulus*. The bodies of the sacral vertebrae are roughly equivalent in craniocaudal length in *Indohyus* and pakicetids. Dimensions of the sacrum (RR 156) are as follows: craniocaudal length of S1 is 17.3 mm, craniocaudal length of S2 is 17.8 mm, craniocaudal length of S3 is 16.9 mm, total sacrum craniocaudal length is 57.2 mm, S2 dorsoventral height is 22.8 mm and S3 dorsoventral height is 24.1 mm.

Caudal vertebrae

Processes on the caudal vertebrae of *Indohyus* (RR 339, Figure 2.8–2.9; RR 294, Figure 2.10) are gracile, unlike the long and robust processes of pakicetids (H-GSP 96557). Compared to *Indohyus*, *Tragulus* displays relatively larger processes that extend farther laterally and are mediolaterally wider. The processes of pakicetids, whose processes remain close to the vertebral body, lack a dorsal projection. *Indohyus* (RR 169, 294,304) and *Diacodexis* (USGS 2352) have relatively large cranial transverse and hemal processes compared to pakicetids and *Tragulus*. The cranial articular processes of *Indohyus* (RR 294) and pakicetids (H-GSP 96557) are medially-directed while those of *Tragulus* are dorsally-directed. The mammillary processes of *Indohyus* and pakicetids are robust and prominent compared to the absence of these processes in *Tragulus*.

Terminal caudal vertebrae and their processes of *Indohyus* (e.g. RR 294) are relatively smaller, as in *Diacodexis* (USGS 2352, Rose 1985; Thewissen and Hussain 1990) and pakicetids (Madar 2007). The caudalmost vertebrae of *Tragulus* lack these processes. Dimensions of the middle (RR 294, Figure 2.11) caudal vertebra are as follows: proximodistal length is 33.0 mm, mediolateral width is 26.5 mm and dorsoventral height is 14.7 mm. Dimensions of the terminal caudal vertebra (RR 249) are as follows: proximodistal length is 26.0 mm, mediolateral width is 11.4 mm and dorsoventral height is 6.4 mm.

Scapula

The glenoid fossa of *Indohyus* (RR 155, Figure 3.1–3.2; RR 263, Figure 3.3) is slightly concave, as in pakicetids (H-GSP 96507, 96532; Madar 2007), but less concave than the glenoid fossae of *Diacodexis* (Rose 1985) and *Tragulus* (CMNH 21826). The glenoid fossa is triangular in cross-section in *Indohyus*, but rounded in cross-section in pakicetids, *Diacodexis* and *Tragulus*. The cranial border of the fossa projects ventrally in *Indohyus* and pakicetids, while in *Diacodexis* and *Tragulus* the cranial border is relatively flattened. The scapulae of both *Indohyus* and pakicetids display a prominent supraglenoid tubercle, while in *Diacodexis* and *Tragulus* the tubercle is smaller. The coracoid process of *Indohyus* is bulbous in cross-section and projects medially, while in both pakicetids and *Tragulus* this process is hook-shaped with the tip directed medially. A prominent scapular spine runs the proximodistal length of the lateral portion of the scapula of *Indohyus*. This spine bears a large projection in *Indohyus* and pakicetids (Madar 2007). In *Indohyus*, the distal end of the spine terminates into an acromion process that is directed cranially at its tip. In contrast, the acromion process of pakicetids, *Diacodexis* and *Tragulus* is oriented closer to a vertical plane with the scapular spine. Only the distal part of the supraspinous fossa of *Indohyus* is preserved. There are no accessory spines. In *Indohyus*, the portion of this fossa contributing to the scapular neck faces laterally, and this fossa is probably larger than the infraspinous fossa. Measurements of the glenoid of RR 155 are as follows: craniocaudal width is 14.9 mm and mediolateral width is 11.4 mm.

Humerus

Humeri of *Indohyus* (RR 149, Figure 3.4, 3.5, 3.10–3.11), *Diacodexis* (USGS 2352; Rose 1985) and *Tragulus* (CMNH 17917) are long and gracile relative to those of pakicetids. The proximal humeral epiphysis of *Indohyus* has relatively small tuberosities for the attachment of muscles originating from the scapula. The proximal humeral shaft is broad, but the distal portion of the shaft is narrow. The distal epiphysis is broad with large radial and ulnar facets, including a deep olecranon fossa.

Indohyus and pakicetids (H-GSP 30128) display a large subspherical head on the proximal humeral epiphysis (Figure 3.4, 3.10), while *Tragulus* (CMNH 17917) displays a hemispherical humeral head. In *Indohyus* and *Tragulus* the greater tuberosity flanks the cranial surface of

the humeral head, and extends well above the humeral head, but the tuberosity is smaller in pakicetids (Madar 2007). In *Indohyus*, the lesser tuberosity flanks the medial surface of the humeral head, is level with the humeral head and shares part of its surface with the humeral head. The lesser tuberosity of pakicetids and *Tragulus* is also low, but is separate from the humeral head.

The humeral shaft of *Indohyus*, *Diacodexis* and *Tragulus* is broadest in its proximal portion, and the distal portion of the shaft is elliptical in cross-section. In contrast, pakicetids display a humeral shaft with a narrow proximal portion and broader distal portion (Madar 2007). *Indohyus* may display a deltopectoral crest as it is tentatively identified in a single specimen (RR 145). *Diacodexis* lacks this crest, but it is present in pakicetids (H-GSP 92042; Madar 2007) and *Tragulus*.

The distal epiphysis of the humerus of *Indohyus* (Figure 3.11) is intermediate in size between the large epiphysis of pakicetids and the narrow epiphysis of *Tragulus*. In *Indohyus* the epicondyles are small; the medial epicondyle is larger than the lateral, and both are slightly larger relative to those of *Tragulus*. In contrast, the epicondyles of pakicetids are much larger than either those of *Indohyus* or *Tragulus*. As in pakicetids and *Tragulus*, the medial epicondyle of *Indohyus* (RR 145) displays a depression for the attachment of the humeral-ulnar ligaments, a caudal projection for the attachment of the flexor muscles, and an intercondylar ridge between the capitulum and epicondyle (RR 145, 149). The distal humeral epiphysis of *Indohyus* displays a flattened entepicondyle and lacks an epicondylar foramen. A deep olecranon fossa perforates the shaft to form a supratrochlear foramen in *Indohyus* (RR 145, 149) and *Tragulus*, but not in pakicetids. The trochlea and capitulum of the epiphysis are preserved but slightly deformed. The trochlea bears a central shallow groove and a medial crest that forms the medial boundary of the olecranon fossa. The capitulum bears a sharp crest on its lateral surface that extends proximally to the trochlea in both *Indohyus* and pakicetids, but is distal to the trochlea in *Tragulus*. Dimensions of the humerus (RR 149) are as follows: proximodistal length is 110.6 mm, proximal epiphysis craniocaudal width is 10.6 mm, proximal epiphysis mediolateral width is 17.5 mm, midshaft mediolateral width is 8.7 mm, midshaft craniocaudal width is 4.9 mm, distal epiphysis mediolateral width is 16.3 mm, distal epiphysis craniocaudal width is 11.2 mm, olecranon fossa mediolateral width is 5.5 mm, olecranon fossa proximodistal length is 6.4 mm, trochlea mediolateral width is 8.9 mm and capitulum mediolateral width is 2.4 mm.

Radius

The radius of *Indohyus* (RR 265, RR 336, Figure 3.6–3.7) is elliptical in cross-section with a wide mediolateral axis and thin dorsoventral axis. The craniodistal portion of the radius bears a longitudinal depression for the attachment of the extensor muscles of the manus (RR 36, 265; Figure 3.6). Pakicetids only display a slight extensor depression, and in *Tragulus* (CMNH 17917, 21026) this depression is located along the craniomedial part of the distal radius and is directed medially. The caudal portion of the radius is concave to accommodate the attachment of the deep flexor muscles in *Indohyus* (RR 36, 265), pakicetids (H-GSP 30324, 96595, 96061, 96228, 98191; Madar 2007), *Diacodexis* (USGS 2352; Rose 1985) and *Tragulus* (CMNH 17917, 21826). The distal part of the radius (RR 265, 336) bears two facets (scaphoid facet (medial), and lunate facet (lateral)) for articulation with carpal elements (Figure 3.7) that are small compared to those of pakicetids, *Diacodexis* and *Tragulus*. Measurements of the radius (RR 265) are as follows: distal epiphysis mediolateral width is 11.2 mm, distal epiphysis craniocaudal width is 5.9 mm and length of the extensor depression is 18.4 mm.

Ulna

The ulna of *Indohyus* is separate from the radius along its entire length. The ulna is mediolaterally compressed, and its caudal edge is concave. The distal portion of the ulna is not preserved in any *Indohyus* specimens.

Compared to *Indohyus* (Figure 3.8–3.9), the proximal portion of the olecranon is more robust in the pakicetids *Pakicetus* (H-GSP 96057) and *Nalacetus* (H-GSP 30286). Compared to *Indohyus*, the olecranon of *Tragulus* (CMNH 17917) extends farther in the proximal direction, its caudal surface lacks a distally-projecting slope and the apex of the process is capped by large, rounded tuberosities. The semilunar notch of *Indohyus* (RR 39, 144) is shallow and displays small anconeal and coronoid processes compared to those of pakicetids (H-GSP 30286). Two radial facets are present on the ulna of *Indohyus* (RR 144), but they are fragmentary.

Magnum

A single magnum is preserved for *Indohyus* (RR 250; Figure 3.12–3.13), but this bone has not yet been recovered in pakicetids (Madar 2007), and is fused with other carpals in *Tragulus*. The magnum of *Indohyus* was therefore compared with the magnum of *A. natans* (H-GSP 18507, Thewissen et al. 1996).

The proximal surface of the magnum of *Indohyus* bears a large, teardrop-shaped facet for articulation with the lunate, as well as a more medially placed and smaller facet for articulation with metacarpal IV. The lunate facet of the magnum has a wide cranial surface and tapered caudal surface in *Indohyus* (Figure 3.13), as in *Ambulocetus*. The cranial surface of the magnum is flat and broad (Figure 3.12), while in *Ambulocetus* it is hourglass-shaped and concave. The medial surface of the *Indohyus* magnum is broad and concave for articulation

with the unciform, while the lateral surface is smaller and bears a small facet for articulation with the trapezoid. The unciform and magnum are fused in *Ambulocetus*. In both *Indohyus* and *Ambulocetus*, the caudal portion of the magnum is extremely tapered and bears a caudodistal projection. In *Indohyus*, the distal part of the magnum bears a teardrop-shaped and convex facet for articulation with metacarpal III. Dimensions of the magnum (RR 250) are as follows: proximodistal length is 5.7 mm, cranial surface mediolateral width is 4.6 mm and caudal surface mediolateral width is 0.9 mm.

Metacarpals

Metacarpals of *Indohyus* are distinguished from metatarsals by their relatively short length, narrow width and deep shaft. Identification of specific elements is based on the shape of the proximal epiphysis.

Metacarpal shafts of *Indohyus* (Figure 4.1–4.3) and pakicetids (Madar 2007) are separated, while those of *Tragulus* (CMNH 17917) and other ruminants are fused. Metacarpal I of *Indohyus* (RR 297, Figure 4.1) is the shortest metacarpal. This metacarpal bears a proximal facet that is rectangular and convex in the dorsoplantar axis, but the presence of two prominent ridges flanking the medial and lateral portions of the facet makes it concave in the mediolateral axis. The distal facet of metacarpal I of *Indohyus* is asymmetrical, and its plantar surface bears a sagittal crest. Metacarpals II and V of *Indohyus* were not preserved. Central metacarpals (III and IV) are robust in both *Indohyus* (Figure 4.2–4.3) and pakicetids. The proximal facets of metacarpals III and IV of *Indohyus* (RR 228, 271) and pakicetids (H-GSP 92041, 96424) are convex with the plantar portion of the facet sloping in the distal direction. In both taxa, the longitudinal axis of the proximal facets is oriented craniocaudally. This facet spans the entire mediolateral width of the metacarpals in pakicetids (H-GSP 92041) and *Tragulus*, but in *Indohyus* (RR 228) it is flanked along its medial and lateral edges by prominent ridges that limit mediolateral translation of the unciform and trapezoid. Shafts of these metacarpals gently widen distally, and the head is only slightly wider than the shaft in both *Indohyus* (RR 83, 138, 199, 228, 271) and *Tragulus*. In contrast, the metacarpal head of pakicetids is bulbous (H-GSP 96315, 98187). In *Indohyus*, the dorsal surface of the metacarpal head is large and smooth, while the plantar surface bears a sagittal crest. Dimensions of a metacarpal III (RR 271) are as follows: proximodistal length is 34.1 mm, proximal epiphysis mediolateral width is 4.6 mm, proximal epiphysis craniocaudal depth is 5.5 mm, midshaft mediolateral width is 4.0 mm, midshaft craniocaudal depth is 3.3 mm, distal epiphysis mediolateral width is 5.0 mm and distal epiphysis craniocaudal depth is 6.1 mm. Dimensions of another metacarpal III (RR 228) are as follows: proximodistal length is 38.1 mm, proximal epiphysis mediolateral width is 5.3 mm, proximal epiphysis craniocaudal depth is 6.9 mm, midshaft mediolateral width is 4.5 mm, midshaft craniocaudal depth is 3.7 mm, distal epiphysis mediolateral width is 7.7 mm and distal epiphysis craniocaudal depth is 4.4 mm. Dimensions of other metacarpals are listed in Table 1.

Table 1. *Indohyus* metapodial and phalangeal length measurements. Lengths marked with an ∗ indicate an incomplete total bone length.

Bone	Specimen	Length (mm)
Manus		
Metacarpal, central	RR 10	38.8
Metacarpal, central	RR 278	33.7
Metacarpal, peripheral	RR 69	25.5∗
Metacarpal, peripheral	RR 83	36.7
Metacarpal I	RR 297	22.3∗
Metacarpal III, left	RR 138	31.7
Metacarpal III, left	RR 228	38.1
Metacarpal III, left	RR 271	34.0
Metacarpal IV, left	RR 270	35.5
Phalanx, central, proximal	RR 273	19.0
Phalanx, central, proximal	RR 274	18.0
Phalanx, central, proximal	RR 281	21.4
Phalanx, peripheral, proximal	RR 177	16.7
Phalanx, intermediate	RR 99	12.9∗
Phalanx, intermediate	RR 117	14.0∗
Phalanx, intermediate (juvenile)	RR 179	14.4∗
Phalanx, digit I, intermediate	RR 233	9.3∗
Phalanx, digit I, intermediate	RR 234	10.2
Phalanx, digit I, intermediate	RR 308	8.2
Pes		
Metatarsal, peripheral	RR 8	48.9
Metatarsal, peripheral	RR 47	26.4∗
Metatarsal, central	RR 76	22.2∗
Metatarsal, peripheral	RR 88	55.4
Metatarsal, central	RR 291	14.1∗
Metatarsal, central	RR 105	31.2∗
Metatarsal III, right	RR 139	57.6
Metatarsal, central	RR 158	68.3
Metatarsal, peripheral	RR 199	30.1
Metatarsal IV, left	RR 225	63.4
Phalanx, central, proximal	RR 26	33.9
Phalanx, central, proximal	RR 37	35.1
Phalanx, central, proximal	RR 118	26.7∗
Phalanx, central, proximal	RR 126	23.8
Phalanx, central, proximal	RR 132	31.2
Phalanx, peripheral, proximal	RR 172	25.6
Phalanx, peripheral, proximal	RR 91	25.9
Phalanx, peripheral, proximal	RR 200	27.6
Phalanx, peripheral, proximal	RR 231	26.2
Phalanx, peripheral, proximal	RR 236	21.6
Phalanx, peripheral, proximal	RR 275	29.2
Phalanx, peripheral, proximal	RR 293	18.4∗
Phalanx, intermediate	RR 19	20.8
Phalanx, intermediate	RR 34	14.2
Phalanx, intermediate	RR 114	17.1
Phalanx, intermediate	RR 125	17.2
Phalanx, intermediate	RR 181	19.7
Phalanx, intermediate	RR 230	17.7
Phalanx, intermediate	RR 276	18.6
Phalanx, intermediate	RR 277	18.2

Phalanges of the manus

No terminal phalanges of the manus were found. Proximal and intermediate phalanges of the manus of *Indohyus* can be distinguished from pedal phalanges based on their small size.

Only proximal phalanges of the central digits of the manus are preserved (Figure 4.4–4.6). These phalanges are relatively conical in shape, smaller than metacarpals, the head is much smaller than the proximal epiphysis, and their shapes are similar to those of *Diacodexis* (AMNH 27787), but are gracile compared to those of pakicetids (H-GSP 92103, 96592) and *Tragulus*. In *Indohyus*, the proximal epiphyses of these phalanges are hemispherical in shape with a groove along their craniocaudal surface for articulation with the sagittal crest of the metacarpal head. Raised medial and lateral edges of this facet cradle the sagittal crest. These raised edges are more pronounced and sharper in pakicetids (H-GSP 96592) and *Tragulus* (CMNH 21826) compared to those of *Indohyus* (RR 273, Figure 4.5). In *Indohyus*, the distal facets of the phalanges are trochleated with a central groove extending along the dorsopalmar portion of the facet. Dimensions of a proximal phalanx (RR 281) are as follows: proximodistal length is 21.5 mm, mediolateral width of proximal facet is 5.0 mm, craniocaudal depth of the proximal facet is 6.3 mm, midshaft mediolateral width is 2.6 mm, midshaft craniocaudal width is 3.7 mm, mediolateral width of distal facet is 2.8 mm and craniocaudal depth of the distal facet is 3.2 mm. Dimensions of other elements of the manus are listed in Table 1.

Intermediate phalanges of digit I, and the central digits, are preserved for *Indohyus*. Intermediate phalanges of *Indohyus* are conical in shape, shorter than the proximal phalanges and the head is considerably smaller than the proximal epiphysis. Compared to the central intermediate phalanges (RR 99, 117), intermediate phalanges of digit I of *Indohyus* (RR 233, 234,308) are considerably smaller and bear a relatively wider head (Figure 1.7). The central intermediate phalanges of *Indohyus* bear a proximal epiphysis that is relatively wider compared to that of *Diacodexis* (AMNH 27787). Central intermediate phalanges are also narrow and gracile compared to the robust and rectangular-shaped phalanges of a pakicetid (H-GSP 96177) and *Tragulus* (CMNH 17917). In *Indohyus*, the proximal facet bears two mediolateral concavities separated by a crest for articulation with the trochlea of the proximal phalanx. The distal facet bears a trochlea. Dimensions of the intermediate phalanx (RR 117) are as follows: proximodistal length is 14.5 mm (specimen lacks distal epiphysis), mediolateral width of proximal facet is 5.0 mm, craniocaudal depth of the proximal facet is 3.8 mm, midshaft mediolateral width is 3.4 mm and midshaft craniocaudal width is 2.1 mm. Dimensions of other manual elements are listed in Table 1.

Pelvis

The innominate of *Indohyus* (Figure 5.1, 5.2) most closely resembles that of the pakicetid *Nalacetus* (H-GSP 30395; Madar 2007). The ilium of *Indohyus* is generally flat with a robust neck and its cranial extension bears a wide blade (RR 44, 257). The medial surface of this blade bears an irregular surface indicating the presence of a sacroiliac joint (RR 43, 162). The iliac neck of *Indohyus* is similar to that of *Nalacetus* (H-GSP 30395) in being flattened mediolaterally (RR 44, 256, 259), while the iliac necks of *Diacodexis* and *Tragulus* are flattened dorsoventrally. *Indohyus* bears a prominent anterior inferior iliac spine for the origin for the rectus femoris muscle (Rose 1985), just cranial to the acetabulum (RR 43, 256, 257, 259). The inferior iliac spine of *Indohyus* is smaller compared to that of *Nalacetus*, similar to that of *Diacodexis*, and larger than the tiny tuberosity of *Tragulus*. A depression is found adjacent to the anterior inferior iliac spine in *Indohyus* (RR 257). The iliac blades of *Indohyus* (RR 257) and *Pakicetus* (H-GSP 30213; Madar 2007) are longer and deeper and bear concave lateral (gluteal) and convex (auricular) surfaces.

The ischia of *Indohyus* (RR 256; Figure 5.1) and *Nalacetus* (H-GSP 30395) are robust and elliptical, compared to the gracile and triangular cross-sectioned ischia of *Tragulus* (CMNH 17917). A broad dorsomedial extension of the ischial body is only present in a single specimen of *Indohyus* (RR 257; Figure 5.2) and displays a series of parallel, caudally directed rugosities. The ischial tuberosity is robust and prominent in *Indohyus* (RR 257) and greater in size compared to that of *Tragulus*. The dorsocaudal margin of the ischium displays a sharp dorsal curvature, the tip of which is the ischial tuberosity, in *Indohyus* (RR 256) and *Nalacetus*, whereas this curvature is absent in *Diacodexis* and *Tragulus*.

Acetabulae of *Indohyus* (RR 43, 146, 256, 259), *Nalacetus* and *Pakicetus* are shallow and elliptical in cross-section with a long craniocaudal axis, while those of *Diacodexis* and *Tragulus* are deeper and spherical. *Indohyus*, *Nalacetus* and *Pakicetus* display prominent dorsocaudal and flattened ventral rims of their acetabulae, unlike the wholly sharp-rimmed acetabulum of *Tragulus*.

The obturator foramen (Figure 5.1) is large in *Indohyus*, *Nalacetus*, *Pakicetus* (Thewissen et al. 2009) and *Diacodexis*, relative to that of *Tragulus*. Relative to the other compared taxa, the obturator foramen of *Tragulus* is smaller craniocaudally as the caudal surface of this foramen is positioned closer to the acetabulum.

Innominates of *Indohyus* can be separated into gracile (RR 43, 44, 162, 256; Figure 5.1) and robust (RR 146, 257, 258, 259; Figure 5.2) forms. The gracile forms are thinner and display two tuberosities separated by a deep depression for muscle attachment located cranially to the acetabulum. Robust forms only display one of these tuberosities, the anterior inferior iliac spine. Gracile forms

also display little to no dorsal shelf to the ilium and ischium, while robust forms display a medial-projecting, shelf-like, dorsal surface that is thick and has marked rugosities consistent with muscle attachment. These differences in morphology could be attributed to sexual dimorphism, but further specimens are needed to confirm this hypothesis.

Dimensions of the innominate (RR 256) are as follows: acetabulum craniocaudal length is 14.6 mm, acetabulum dorsoventral width is 13.9 mm, obturator foramen craniocaudal length is 37.7 mm and obturator foramen dorsoventral width is ~19.0 mm.

Femur

The femoral head of *Indohyus* (Figure 5.3–5.5) is oval in shape with a long mediolateral axis (RR 42, 101, 264), as in *Tragulus* and *Pakicetus* (H-GSP 30333; Madar 2007). The greater trochanter of the femur of *Indohyus* is prominent, extends slightly proximal to the proximal surface of the femoral head and its intertrochanteric crest connects with the triangular-shaped lesser trochanter (RR 42, 89, 101, 154, 161, 237, 267), like that of *Diacodexis*, *Tragulus* and *Pakicetus* (H-GSP 30345). A deep trochanteric fossa is present in *Indohyus* (RR 42, 101, 154, 237). The greater trochanter of *Indohyus* is relatively larger than the lesser trochanter (RR 42, 89, 101, 161, 267), as in *Diacodexis* and *Tragulus*. The greater trochanter of *Indohyus* is relatively smaller compared to that of pakicetids, but is equivalent in size to that of *Tragulus*. In *Indohyus* and pakicetids, the lesser trochanter projects from the proximal portion of the femoral shaft. The third trochanter of the femur of *Indohyus* projects from approximately one-third of the femoral shaft length and is smaller than that of *Pakicetus* (H-GSP 30345), but greater than that of *Diacodexis* and *Tragulus*.

The femoral shaft (Figure 5.3–5.5) of *Indohyus* is thicker compared to that of *Diacodexis* (USGS 2352; Rose 1985) and *Tragulus* (CMNH 17917). The shaft is elliptical in transverse section and is wider mediolaterally rather than craniocaudally in *Indohyus* (RR 42, 154, 161, 267, 340), while in *Diacodexis* the proportions are reversed, and in *Tragulus* the shaft is circular in cross-section.

The distal end of the femur of *Indohyus* (RR 101, Figure 5.3–5.4; RR 133, Figure 5.6) is wider compared to that of *Diacodexis* and *Tragulus*. The patellar groove of the femur of *Indohyus* is shallow with slightly raised margins (RR 101), unlike the sharp and deepened grooves of *Diacodexis* and *Tragulus*. The medial epicondyle of the femur is a raised globular projection in *Indohyus* (RR 101) and *Diacodexis*, and a crest in *Tragulus*. The lateral epicondyle of the femur is a raised rugose area in *Indohyus* (RR 101), *Diacodexis*, and *Tragulus*. The distal extent of these condyles is equivalent in a single specimen of *Indohyus* (RR 101), but the lateral condyle extends farther distally than the medial condyle in another specimen of *Indohyus* (RR 133), *Diacodexis* and *Tragulus*. The lateral condyle is wider than the medial condyle as in *Diacodexis* and *Tragulus*. A distinct round pit, the extensor fossa, is located at the junction of the lateral ridge of the patellar groove and the lateral epicondyle. This fossa is smaller in *Indohyus* (RR 101), and is much deeper in *Diacodexis* and *Tragulus*. The extensor fossa serves as the attachment for the m. extensor digitorum longus. Dimensions of the femur of *Indohyus* (RR 101) are as follows: proximodistal length is 120.1 mm, midshaft mediolateral width is 11.7 mm, midshaft craniocaudal width is 7.3 mm, femoral head mediolateral diameter is 15.0 mm, patellar groove length is 26.7 mm and patellar groove width is 9.7 mm.

Patella

The patella of *Indohyus* (RR 269, RR 333; Figure 5.13) has a convex cranial surface and a concave acaudal surface as in *Diacodexis* (USGS 2352; Rose 1985). The proximal end of the patella is thicker than the distal end in both the craniocaudal and mediolateral dimensions. The caudal surface of the patella displays two longitudinal depressions located on its medial and lateral portions. Patellar dimensions (RR 269) are as follows: mediolateral width is 11.3 mm, proximodistal length is 16.5 mm, maximum craniocaudal width (along proximal part of patella) is 6.7 mm and minimum craniocaudal width (along distal part of patella) is 2.6 mm.

Tibia

The tibia of *Indohyus* (Figure 5.7–5.10) is triangular in transverse section (RR 46, 84). The proximal articular surface (Figure 5.7–5.8) bears a large lateral condyle and a smaller medial condyle for articulation with the femur (RR 22, 84), as in *Diacodexis* (USGS 2352; Rose 1985) and *Tragulus* (CMNH 17917). In *Pakicetus* (H-GSP 30357), the lateral condyle is relatively larger than that of *Indohyus*. In *Indohyus*, these condyles are convex in the craniocaudal direction and concave in transverse section (RR 22). *Indohyus* (RR 22, Figure 5.8) displays small central spines that separate the condyles, unlike the large and prominent spines of *Pakicetus* (H-GSP 30357) and *Tragulus*. The lateral condyle bears a deep sulcus along its cranial and medial-most border that accommodates the long digital extensors in *Indohyus* (RR 84), *Pakicetus*, *Diacodexis* and *Tragulus*. Below the caudal and distal-most portion of the lateral condyle lies an ovoid depression for the fibular head as in all examined taxa. The tibial tuberosity of *Indohyus* (Figure 5.7) is more robust in its mediolateral width than in *Diacodexis* and *Tragulus*. Continuing distally from this tuberosity is the tibial crest of *Indohyus* (RR 143, Figure 5.9), which forms the medial

border of the fossa for the attachment of the tibialis cranialis muscle. This fossa continues approximately 20–25% down the tibial shaft in *Indohyus* (RR 143), *Diacodexis* and *Tragulus*, but is longer, occupying approximately 40% of the shaft in pakicetids (H-GSP 30357). The popliteal fossa is deepest in the tibia of *Indohyus* (RR 84) and *Pakicetus* (H-GSP 30357), whereas in *Diacodexis* and *Tragulus* this fossa is shallow. The astragalar facet of the tibia is rectangular and is longest in the craniocaudal plane in *Indohyus* (RR 301, Figure 5.10), while this facet is approximately square in pakicetids (H-GSP 30357), and *Tragulus*. A sagittal crest divides a larger lateral trochlear facet and narrow medial trochlear facet in *Indohyus* and pakicetids. *Tragulus* bears a relatively larger medial facet. The lateral and distal surface of the tibia of *Indohyus* displays a triangular concavity for articulation with the fibula that is relatively larger in pakicetids (H-GSP 30357) and absent in *Tragulus*. The medial malleolus of *Indohyus* is blunt, distally-directed and bears a flattened articular surface, whereas in *Tragulus*, the malleolus curves laterally and the facet is saddle-shaped. The cranial and caudal surfaces of the distal epiphysis of the tibia of *Indohyus* display two small, triangular projections. In *Tragulus*, these projections are comparatively large and curve towards the centre of the epiphysis. Dimensions of the proximal end of the tibia (RR 84) are as follows: tibial plateau mediolateral width is 27.5 mm and craniocaudal width is 24.0 mm; tibial crest mediolateral width is 5.3 mm; shaft mediolateral width is 12.9 mm; craniocaudal width is 14.3 mm. Dimensions of the distal part of the tibia are as follows: distal epiphysis mediolateral width is 10.0 mm, craniocaudal length is 13.2 mm and proximodistal length of the medial malleolus is 4.6 mm from the centre of the distal epiphysis.

Fibula

Based on the presence of several incomplete fibulae and fibular facets on the tibia and astragalus of *Indohyus*, the fibula was complete, lacked proximal tibial fusion and was a slender rod relative to the tibia, as in pakicetids (Madar 2007) and *Diacodexis* (USGS 2352, Rose 1985). The presence of a fibula in *Tragulus* is variable with some individuals retaining only vestiges that are fused to the tibia (Rose 1985). The proximal articular surface of the fibula of *Indohyus* (Figure 5.11) slopes with a distal-projecting medial surface and fits into the fibular facet of the tibia (RR 84), but is flattened in a different specimen (RR 334). The distal end of the fibula (Figure 5.12) widens to a large teardrop-shaped facet. Dimensions of the proximal part of the fibula (RR 96) are as follows: shaft mediolateral width is 4.1 mm, shaft craniocaudal width is 2.8 mm, proximal facet mediolateral width is 6.6 mm and proximal facet craniocaudal width is 2.7 mm.

Astragalus

The astragalus (Figure 6.1–6.3) of *Indohyus* is gracile, like that of pakicetids (H-GSP 30153, 98148; Madar 2007), but unlike the more robust astragalus of *Tragulus* (CMNH 21826). The astragalar neck of *Indohyus* and pakicetids is long along its proximodistal axis, but smaller in *Tragulus*. As in all artiodactyls, the astragalar head is trochleated. Both trochleae are oriented in a vertical plane in *Indohyus* (RR 129, 213, 224, 246, 290), *Tragulus* and some pakicetids (H-GSP 98148), but trochleae are offset in *Diacodexis* (Rose 1985) and another specimen of pakicetids (H-GSP 30153). The proximal portion of the astragalus is deeply trochleated while the distal end bears a shallower trochlea in *Indohyus* (RR 129, 213, 224, 246), similar to pakicetids (Madar 2007), *Tragulus* (CMNH 21826) and *Diacodexis* (Thewissen and Hussain 1990).

The lateral surface of the lateral condyle of the tibial trochlea of *Indohyus* is concave but bears two ectal facets for articulation with the calcaneus and a fibular facet. The ectal facet (Figure 6.1–6.3) is elliptical in *Indohyus* (RR 35, 224), pakicetids (H-GSP 31053, 98148) and *Diacodexis* (Gingerich et al. 2001), but conical in *Tragulus* (CMNH 21826). The ectal facet is plantar-facing in *Indohyus* (RR 35, 224) and pakicetids (H-GSP 30153, 98149; Madar 2007). The plantar ectal facet (Madar 2007) lies along the cranial and distal portions of the lateral condyle and is only found in *Indohyus* (RR 35, 224, 246) and pakicetids (Madar 2007). The lateral surface of the lateral condyle of the tibial trochlea of *Indohyus* also has a sharpened rim and a slightly concave surface for articulation with the distal part of the fibula.

The distal trochlea of the astragalus of *Indohyus* bears a lateral facet for articulation with the cuboid. This cuboidal facet is narrower mediolaterally compared to the medial condyle (navicular facet) in all examined taxa and the facet forms a right angle with the parasagittal plane. A sharp crest separates these facets.

The sustentacular facet of the astragalus of *Indohyus* (Figure 6.3), located along the caudal surface of the astragalar neck, is saddle-shaped with a slightly raised lateral ridge in all examined taxa. This facet covers 78% of mediolateral width of the astragalus in *Tragulus*, but is mediolaterally smaller in *Indohyus* (RR 224) and *G. pakistanensis* (sustentacular facet width is 57% of astragalar width) and pakicetids (43–50% of the astragalar width, H-GSP 30153, 98148). The lateral edge of the sustentacular facet of *Indohyus* lies in line with the lateral margin of the tibial trochlea, and the distal part of this facet is completely separated from the cuboid and navicular facets. Dimensions of the astragalus (RR 224) are as follows: mediolateral width is 10.8 mm, proximodistal length is 20.3 mm, craniocaudal width is 12.3 mm, proximodistal length of neck is 6.2 mm and the sustentacular facet is 6.8 mm in mediolateral width.

Calcaneus

The calcaneus of *Indohyus* (Figure 6.4–6.6) is very narrow mediolaterally, like that of *Diacodexis* (USGS 2352, Rose 1985) and pakicetids (Madar 2007). A deep fossa (for the attachment of calcaneofibular ligaments) excavates the lateral surface, and encompasses the distal two-thirds of the lateral surface in *Indohyus* (RR 164, 170), the distal half in *Diacodexis*, and may extend the entire length of the lateral surface in pakicetids (Madar 2007). The tuber calcis, located at the proximal apex of the calcaneus, displays a taller medial tuberosity and flattened lateral tuberosity in *Indohyus* (RR 167, 170) as in *Diacodexis*, *Tragulus* and the pakicetid *Ichthyolestes* (H-GSP 92063). The sustentaculum tali, which articulates with the sustentacular facet of the astragalus, bears a smaller ovoid facet in *Indohyus* (RR 164, 170). This facet is relatively robust in *Tragulus*. The fibular facet along the cranial part of the calcaneus is rounded and bears a prominent hemispherical facet for articulation with the fibula in *Indohyus* (RR 164) and pakicetids (H-GSP 30246, 92063, 96612). The cuboidal facet, located along the caudal and distalmost portion of the bone, is elliptical in outline as in *Tragulus* (CMNH 21826), but is smaller craniocaudally compared to some pakicetids (H-GSP 30246, 96612). This facet forms a steep angle at the distal portion of the calcaneus in all examined taxa. Dimensions of the calcaneus (RR 167) are as follows: proximal distal length is 41.0 mm, mediolateral width at the tuber calcis is 7.44 mm, mediolateral width at base of calcaneal tuber is 5.8 mm, proximodistal length of calcaneal tuber is 22.3 mm and the medial extent of sustentaculum tali from calcaneal tuber is 5.3 mm.

Cuboid

The cuboid of *Indohyus* (RR 214, Figure 6.7–6.9) is hourglass shaped in dorsal view, as in pakicetids (H-GSP 30174, Madar 2007). The proximal surface of the cuboid bears two facets, an astragalar facet and a larger calcaneal facet. Only the cranial portion of the astragalar facet is preserved. The calcaneal facet of the cuboid of *Indohyus* is sloped distally and is large along its mediolateral portion, as in pakicetids and *Tragulus* (CMNH 21826). Along the cranial edge of the medial surface of the cuboid of *Indohyus* is a broken prominence for articulation with the navicular, as in pakicetids (H-GSP 30174, Madar 2007). Along the caudal part of the medial surface of the cuboid of *Indohyus* is an additional convex facet for articulation with the navicular, but this facet is larger than that of pakicetids. Encompassing most of the cranial and distal borders of the cuboid of *Indohyus* is a large horizontal facet for articulation with metatarsal IV, as in all artiodactyls and pakicetids. This facet is roughly triangular in *Indohyus* and pakicetids (H-GSP 30174), but is arc-shaped in *Tragulus*. A smaller facet for metatarsal V lies along the distal and lateral surface of the cuboid of *Indohyus*, just lateral to the facet for metatarsal I. This facet on metatarsal V is tiny in *Indohyus* and *Tragulus*, but prominent in pakicetids. The caudal and ventral corner of the cuboid of *Indohyus* extends distally to form a plantar process that articulates with the caudal and proximal portions of metatarsal IV, as in *Tragulus*. The plantar process of *Indohyus* is short compared to the long process of pakicetids (Madar 2007). The caudal part of this process is roughly rectangular in *Indohyus*, but v-shaped in pakicetids and *Tragulus*. Cuboid (RR 214) dimensions are as follows: proximodistal length is 10.5 mm, mediolateral width is 7.6 mm and craniocaudal width is 10.6 mm.

Ectomesocuneiform

The ectomesocuneiform of *Indohyus* (RR 192; Figure 6.10) is identified based on a transverse groove along its distal surface to house the tendon of the tibialis posterior muscle. In *Indohyus*, the cranial and caudal surfaces of the ectomesocuneiform are flattened, while the proximal surface displays an hourglass-shaped and flattened facet for articulation with the navicular. Dimensions of the ectomesocuneiform (RR 192) are as follows: craniocaudal length is 7.1 mm; mediolateral width is 5.2 mm and proximodistal length is 5.5 mm.

Metatarsals

Metatarsals of *Indohyus* are distinguished from metacarpals by their greater length, greater mediolateral width, narrow dorsoplantar depth and the presence of a prominent plantar tubercle.

Metatarsals of *Indohyus* (Figure 4.9–4.12, 4.24–4.25), *Diacodexis* (Rose 1985) and pakicetids (Madar 2007) are unfused, whereas these elements are fused in *Tragulus* (CMNH 21826). Compared to pakicetids and *Diacodexis*, the metatarsals of *Indohyus* are more gracile, but are robust in comparison to the metatarsals of *Tragulus*. Presence of metatarsal I is unknown in *Indohyus*, although it could be that RR 199 represents a deformed metatarsal I. The heads of the central metatarsals of *Indohyus* (RR 105, 108, 139, 225, 291) are symmetrical along the base of the shaft, while those of peripheral metatarsals (RR 47, 88, 199) are asymmetrical and steeply sloped mediolaterally. The proximal facets of the central metatarsals (III and IV) of *Indohyus* are concave and rectangular to triangular in outline (RR 158, 225), like the rectangular facets of *Tragulus* (CMNH 21826) and triangular facets of pakicetids. The plantar tubercle is small in the central metatarsals of *Indohyus* (RR 139, 225) but large in those of pakicetids (H-GSP 30405, 30417, 96299). The heads of the distal epiphyses of the metatarsals of *Indohyus* are the widest parts of the central metatarsals, are rounded and convex and their plantar surfaces bear sagittal crests, as in

Diacodexis (USGS 2352) and *Tragulus* (CMNH 21826). This morphology is in strong contrast to the bulbous distal shafts and heads of pakicetids, which are relatively larger in both the mediolateral and craniocaudal dimensions. Dimensions of metatarsal IV (RR 225) are as follows: proximodistal length is 62.2 mm, proximal epiphysis mediolateral width is 6.1 mm, midshaft mediolateral width is 6.3 mm, midshaft craniocaudal width is 4.7 mm and distal head mediolateral width is 10.5 mm. Dimensions of the a central metatarsal (RR 158) are as follows: proximodistal length is 57.8 mm, proximal epiphysis mediolateral width is 5.9 mm, proximal epiphysis craniocaudal depth is 5.9 mm, midshaft mediolateral width is 6.8 mm, midshaft craniocaudal depth is 3.2 mm, distal head mediolateral width is 9.9 mm and distal head craniocaudal depth is 5.9 mm. Additional lengths of other metatarsals are listed in Table 1.

Pedal phalanges

No terminal phalanges of the pes were found for *Indohyus*. Pedal phalanges are tentatively identified based on their larger size relative to the phalanges of the manus. Proximal and intermediate phalanges of the pes of *Indohyus* are distinguished based on the morphology of their proximal epiphyses. Central phalanges of the pes of *Indohyus* are distinguished from peripheral phalanges based on their larger relative size and symmetrical facets.

Proximal phalanges of the pes of *Indohyus* (Figure 4.13–4.16) are conical with a wide proximal epiphysis, narrow distal epiphysis and a midshaft flattened in the dorsoventral plane. The proximal facet of the proximal phalanges is hemispherical in shape, and the facet surface is concave with a central groove for articulation with the sagittal crest of the distal metacarpal. The distal facet of the proximal pedal phalanges is trochleated for articulation with intermediate phalanges. In central proximal phalanges of *Indohyus* (RR 118, 126, 132), both proximal and distal facets are symmetrical about the longitudinal axis of the bone, whereas in phalanges of peripheral digits (RR 91, 200, 231, 236, 275, 293) these facets are asymmetrical. The plantar surfaces of the proximal phalanges display a deep groove along the proximal shaft. The proximal pedal phalanges are more robust than those of *Diacodexis* (USGS 2352), but gracile compared to pakicetids (H-GSP 96593) and *Tragulus* (CMNH 17917, 21826). The distal facet is trochleated. The length of these phalanges is listed in Table 1.

Like proximal phalanges, the intermediate phalanges of the pes of *Indohyus* (Figure 4.17–4.20) are conical in shape and have a distal trochlea, but the intermediate phalanges bear two grooves on their proximal facet for articulation with the distal trochleated facet of a proximal phalanx. Intermediate phalanges are short and narrow compared to proximal phalanges. The length of these phalanges is listed in Table 1.

Discussion

Locomotion

The skeleton of *Indohyus* exhibits a suite of gross morphological characteristics typical of a cursorial artiodactyl adapted to terrestrial locomotion (Rose 1985). Within the vertebral column, the lumbar vertebrae of *Indohyus* have revolute zygapophyses that probably prevented spinal torsion. The appendicular elements of *Indohyus* are gracile and long, like those of a cursorial artiodactyl, with the hindlimbs longer than the forelimbs (Figure 7.3–7.4). The elbow of *Indohyus* probably functioned only in flexion and extension, as its articular morphology appears to have limited the joint's ability to supinate, pronate or undergo mediolateral translation. Greater extension of the ulna of *Indohyus* was probably afforded by the presence of a humeral supratrochlear notch. Within the hindlimb, *Indohyus* also displays the typical artiodactyl characteristic of a tarsus that functioned solely in flexion and extension (Schaeffer 1947), as evidenced by the following morphologies that impede mediolateral joint excursions: a typical double-trochleated astragalus and a tight astragalo-calcaneal articulation that affords limited mediolateral rotation.

Although *Indohyus* displays bone morphologies consistent with terrestrial locomotion, analyses of bone cross-sectional geometries indicate that some parts of the skeleton (i.e. ribs, vertebrae and appendicular elements) were thickened along their endosteal surfaces (osteosclerosis), consistent with the interpretation of a semi-aquatic lifestyle (Figure 7). Pakicetids displayed even greater skeletal osteosclerosis in a greater number of skeletal elements (Gray et al. 2007; Madar 2007). Taken together, morphological data indicate that *Indohyus* could locomote effectively on land, but that its bone cross-sectional geometry suggests an incipient form of an aquatic lifestyle. *Indohyus* thus represents a critical skeletal intermediate between terrestrial artiodactyls that lack alterations to their bone cross-sectional geometry, and the earliest cetaceans (pakicetids) that display alterations to both gross and cross-sectional characteristics of their skeletons.

Vertebral mobility

Indohyus probably held its head well above the thoracolumbar column, while pakicetids oriented the cranium in a horizontal line with their vertebral column, much like crocodilians. This postural difference is suggested by the differences in the cranial and terminal cervical vertebral articulations. Articulated terminal cervical vertebrae of *Indohyus* and *Tragulus* form a steep, superiorly oriented arc to the cervical spine relative to the more craniocaudally oriented thoraco-lumbar portion of the spine. These taxa also display a nearly perpendicular occipitoatlantal articulation, as evidenced

by caudoventrally oriented occipital condyles of the skull and craniodorsal angled facets of the atlas. In contrast to the perpendicular occipitoatlantal articulation inferred for *Indohyus*, the head of *Pakicetus* appears to have been oriented in a much more plane level with the atlas, based on caudally directed occipital condyles and cranially directed facets of the atlas.

Cervical and thoracic vertebrae of *Indohyus* and other artiodactyls are more gracile and display thinner cortices compared to pakicetids (Madar 2007), suggesting that *Indohyus* had relatively less robust axial musculature compared to pakicetids. The lumbar vertebrae of *Indohyus* and most modern artiodactyls have a limited range of mobility in comparison to pakicetids. In most modern terrestrial artiodactyl taxa, the lumbar spine is stiffened by the presence of revolute zygapophyses that impede rotation of individual vertebrae about the longitudinal axis of the column. Revolute zygapophyses are present in all taxa examined here, but pakicetids have zygapophyses that only partially envelop the caudal articular processes of an adjacent vertebra. The zygapophyses of pakicetids encase the ventral and lateral surfaces of the caudal articular surfaces, but only partially encase the dorsal surface, thus allowing limited rotation and greater flexion and extension of the vertebral column compared to terrestrial taxa and *Indohyus*, which may have assisted in swimming.

Caudal vertebrae of *Indohyus* are gracile, probably did not support exceptional caudal musculature and probably did not play a large role during aquatic locomotion compared to those of pakicetids (Madar 2007). Madar (2007) noted that the robust size and enlarged processes of the caudal vertebrae of pakicetids suggested the presence of exceptionally strong epaxial musculature, and concluded that the tail probably acted in concert with the hindlimbs during aquatic locomotion. The gracile vertebrae of *Indohyus* suggest that the tail did not play a major role in generating thrust during aquatic locomotion.

Forelimb mobility

The glenohumeral joint of *Indohyus* may have functioned primarily in facilitating flexion and extension of the humerus, with only a minute amount of mediolateral movement, as in *Odocoileus*. A small mediolateral area of the glenoid suggests this limited mobility. In comparison, *Pakicetus* displayed a glenoid with greater surface area for articulation with the humerus, and thus probably had more mobility in flexion–extension and mediolateral rotation compared to *Indohyus*. The glenohumeral joint of *Tragulus* allowed for the greatest mobility as the humeral head is relatively larger, is hemispherical in shape and displays a greater surface area for the glenoid.

The cubital joint of *Indohyus* may have functioned primarily in flexion and extension, but lacked the ability to supinate and pronate, as in *Diacodexis* (Rose 1985), pakicetids (Madar 2007), *Tragulus* and *Odocoileus*. Both *Indohyus* and *Diacodexis* have a supratrochlear foramen through the distal portion of the humerus, which allowed greater maximum extension of the ulna. This foramen is absent in pakicetids, *Tragulus* and *Odocoileus*.

Metacarpals of *Indohyus* and pakicetids are unfused, but display different apparent ranges of motion in the metacarpophalangeal joints. The distal articular facets of the metacarpals of *Indohyus* display larger dorsal facets, suggesting a greater range of motion in extension and a limited range of motion in flexion. Pakicetids display enlarged distal facets on the metacarpals, and might have been able to equally extend and flex the metacarpophalangeal joint such that the joint could rotate 180°(Madar 2007). This ability for extension is lacking in *Tragulus* and the distal metacarpal mostly facilitates the flexion of the joint.

In *Indohyus* and pakicetids, facets of the first interphalangeal joint suggest a greater range of motion in flexion. The distal trochlea of intermediate phalanges bears only a limited articular surface along the dorsal part, but proximodistally long facets along the plantar surface. The movement of this joint is restricted in *Tragulus* and *Odocoileus* to only a few degrees of flexion or extension.

Forelimb function of *Indohyus* was probably most active in flexion and extension. In the proximal joints (i.e. glenohumeral and cubital), *Indohyus* probably moved like a typical cursorial artiodactyl. Rather than stabilising the metacarpophalangeal and proximal interphalangeal joints along the vertical plane as in modern cursors, *Indohyus* probably extended the metacarpophalangeal joint and flexed the first interphalangeal joint, suggesting a digitigrade posture. Pakicetids are also thought to be digitigrade based on their flat and broad metacarpals and phalanges (Madar 2007).

Hindlimb mobility

The innominates of *Indohyus* and pakicetids display large and flat ischial surfaces that lack the well developed and prominent ischial spine and tuberosity seen on cursorial artiodactyls such as *Odocoileus*. This suggests that *Indohyus* and pakicetids had smaller hamstring musculature compared to terrestrial cursors.

Motion at the femoroacetabular joint of *Indohyus* probably functions mainly in flexion and extension, as in all examined artiodactyls. The acetabulum of both *Indohyus* and *Odocoileus* probably supports extension of the femur to an angle of 45° below the longitudinal axis of the body. The acetabulum of pakicetids and *Tragulus* allows for a greater range of extension. The femur could probably rotate in these taxa until it was parallel to the longitudinal axis of the body. *Indohyus*, *Odocoileus*, pakicetids and *Tragulus* could probably flex the femur

until it was 45°below the longitudinal axis of the body. In all taxa, articulation of the femur and proximal part of the tibia suggest that the knee probably functions primarily in flexion and extension.

The morphology of the proximal tarsus (calcaneus, astragalus and tibia) of all taxa examined indicates that they probably functioned like those of a typical terrestrial artiodactyl in flexion and extension, with only the proximal portion of the calcaneus able to pivot medially during flexion (see Schaeffer 1947; Thewissen and Madar 1999). Taxa can be differentiated from one another based on the astragalo-cuboid joint morphology and on the presence or absence of cubonavicular fusion. *Gujaratia* (Thewissen and Hussain 1990), *Indohyus* and pakicetids (Madar 2007) lack cubonavicular fusion, in contrast to *Tragulus* and *Odocoileus*. Cubonavicular fusion further stabilises the joint and facilitates cursorial and saltatorial locomotion. The position of the astragalo-cuboid joint also varies between these taxa. In some diacodexids, pakicetids and *Indohyus*, the cuboidal facet is positioned proximal to the navicular facet. These taxa also lack metatarsal fusion, and the cuboid and navicular may function independently in facilitating abduction of the metacarpals, corresponding with increasing pedal surface area.

Within the pes, metatarsals and proximal and intermediate phalanges of *Indohyus* are preserved. Unlike the fused metatarsals of *Tragulus* and *Odocoileus*, the metatarsals of *Indohyus* and pakicetids are not synostosed. The morphology of the metatarsophalangeal joints of *Indohyus*, *Tragulus* and pakicetids suggests a greater range of mobility in flexion, rather than in extension, as the distal facet of the metatarsal is longer along its dorsal surface as compared to the ventral surface of the facet. The distal facet of the metatarsal of *Odocoileus* bears a sagittal crest along the entire facet, which probably stabilises the joint against mediolateral translation.

Hindlimb function of *Indohyus* was probably restricted to flexion and extension in hip and knee joints, but the joints of the manus were able to extend and abduct to increase the pedal surface area. Joint angles of both *Indohyus* and pakicetids indicate that the hindlimb was probably digitigrade. Although *Indohyus* was able to locomote on land, its pedal morphology suggests locomotion in either soft substrates (e.g. mud) or pelvic paddling. Both repertoires might have been employed in pakicetids (Madar 2007). However, a hallmark of pelvic paddling is the presence of long metatarsals and phalanges (Thewissen and Fish 1997) and these elements are only slightly longer in *Indohyus* than in terrestrial cursors (e.g. *Odocoileus*, *Tragulus*).

Interdigital webbing

Most modern marine mammals encase the autopod in a soft tissue flipper (see review in Cooper 2009). In cetaceans, this soft tissue flipper has a dermis thickened by dense irregular connective tissue that impedes digital movement and creates a streamlined hydrofoil that generates lift (e.g. Cooper et al. 2008; Weber et al. 2009). Manatees have thick, muscular flippers that function in drag-based propulsion as manatees use them like oars during turning manoeuvres (Hartman 1979). Pinnipeds, walruses and otters, however, have a muscular flipper encased with thin dermal and epidermal layers that afford a large range of motion for the digits. Otariid flippers are oscillated like a bird wing to generate lift (English 1976, 1977), while walruses use their flippers as paddles for steering (Gordon 1981). Otters restrict webbing to their hindlimbs and this additional tissue increases the surface area of the pes increasing the thrust produced by the hindlimbs (Tarassof 1972).

Osteological correlates for this interdigital webbing are thought to occur as flanges along metapodials and phalanges where strong digital abductors attach (Gingerich et al. 2001; Madar 2007). These flanges have been reported in pakicetids (Madar 2007) and protocetids (Gingerich et al. 2001), but are not found in the later occurring basilosaurids (Uhen 2004) and modern cetaceans. This osteological correlate has not been tested in modern taxa as a reliable indicator of strong digital musculature or the presence of interdigital tissues. Indeed, digital abductors are retained in some basal odontocete taxa (i.e., sperm whales (Cooper et al. 2007)) that lack these flanges, and all modern cetaceans display interdigital tissues but lack these flanges.

The metapodials and phalanges of *Indohyus* lack these flanges on their phalanges, perhaps suggesting that either strong abductors were not required for locomotion by *Indohyus*, and/or that they lacked interdigital webbing. If the presence of flanges on phalanges in fact indicates the presence of interdigital musculature and interdigital webbing, webbing may have first evolved in pakicetid cetaceans (Madar 2007), as was documented in protocetids (Gingerich et al. 2001) and could have been a key limb morphology that increased the surface area of the autopod during soft substrate locomotion and swimming manoeuvres.

Hydrostatic strategies

Aquatic tetrapods utilise several strategies to alter their density relative to water (e.g. Kaiser 1960; Wall 1983; Taylor 1993, 2000; de Ricqlès and De Buffrénil 2001; Germain and Laurin 2005; de Buffrénil et al. 2008; Kriloff et al. 2008; Houssaye 2009). These hydrostatic strategies include (see definitions in de Ricqlès and De Buffrénil 2001): osteosclerosis (increased cortical bone thickness along the endosteal surfaces, resulting in a smaller medullary cavity), pachyostosis (increased cortical bone thickness along the periosteal surface, resulting in an enlarged or swollen bone), pachy-osteosclerosis (enlarged bones with a small medullary cavity), osteoporosis (lightening the skeleton by decreasing

cortical bone content and trabecular bone thickness, Wall 1983), ingestion of gastroliths or swallowing stones (Taylor 1993; Wings 2007), lung compression during deep dives (Ridgway and Howard 1979) and the presence of exceptional fat stores (Ling 1974).

Morphologies associated with these hydrostatic strategies can be found in the fossil record. Fossil sirenians had pachy-osteosclerotic ribs (de Buffrénil et al. 2008). The earliest fossil cetaceans had osteosclerotic ribs (pakicetids; Gray et al. 2007) and pachy-osteosclerotic ribs (ambulocetids, remingtonocetids, protocetids and basilosaurids; De Buffrénil et al. 1990, de Ricqlès and De Buffrénil 2001, Gray et al. 2007). Some early mysticetes also display osteosclerotic ribs (some aetiocetids and some Chaeomysticeti; Beatty and Dooley 2009). Some archaeocetes also display osteosclerotic limb bones (pakicetids, ambulocetids, remingtonocetids, protocetids and basilosaurids; Madar 1998, Madar 2007, Thewissen et al. 2007). Although stomach stones have been preserved in several fossil aquatic reptiles (Wings 2007), there is no definitive evidence of fossil aquatic mammals with preserved gastroliths.

Indohyus displays some of the morphologies implicated in hydrostatic control. The long bones (i.e., humerus (RR 157), femur (RR 42), ulna (RR 39), tibia (RR 46), metacarpal (RR 228) and metatarsal (RR 225)), a rib (RR 217) and a caudal vertebra (RR 249) of *Indohyus* have a thickened cortex and small medullary cavity, indicating the presence of osteosclerosis (Figure 7.1–7.7, 7.13). In terrestrial artiodactyl taxa (i.e., modern taxa *Tragulus*, *Saiga*, *Sus* and fossil taxa *Cainotherium*, *Leptomeryx*, *Poebotherium* and *Merycoidodon*) midshaft femoral cross-sections indicate that the medullary cavity takes up 60–75% of the bone diameter, whereas the semi-aquatic *Hippopotamus* has a medullary cavity that takes up 55% of the total bone diameter (Table 2; Thewissen et al. 2007). These results indicate that within the Order Artiodactyla, a semi-aquatic form displays a small medullary cavity when compared to terrestrial forms. *Indohyus* clearly displays femoral osteosclerosis, as the medullary cavity is 42% of the total bone diameter. The earliest cetaceans also displayed osteosclerotic femoral midshafts, although there was variability in the degree of mineralisation. The pakicetids *Nalacetus* and *Ichthyolestes* displayed medullary cavities that were 54 and 25% of the total bone diameter, while *Ambulocetus* displayed a *Hippopotamus*-like bone structure of 57% (Thewissen et al. 2007). Taken together, these results suggest that the femur of *Indohyus* was osteosclerotic relative to terrestrial and semi-aquatic artiodactyls, but its level of osteosclerosis was less pronounced relative to the extreme osteosclerosis seen in the pakicetid archaeocete *Ichthyolestes*.

Similar results were found in an analysis of humeral midshaft dimensions (Figure 7.4, 7.11; Table 2). Terrestrial artiodactyls (i.e. modern taxon *Sus* and fossil taxa *Cainotherium*, *Merycoidodon*, *Oreotragus*) had large medullary cavities that took up 56–93% of the humeral diameter, while the cavity of *Indohyus* encompassed only 48% of the total bone diameter. The pakicetid *Ichthyolestes* had an extremely small cortex (14–16%, Thewissen et al. 2007).

Rib cross-sectional dimensions (Figure 7.7, 7.14) of aquatic tetrapods have been studied in detail (e.g. Fawcett 1942; Domning and Myrick 1980; De Buffrénil et al. 1990; Domning and De Buffrénil 1991; de Ricqlès and De Buffrénil 2001; Uhen 2004; Gray et al. 2007). Aquatic mammals typically display greater mineral content in rib cross-sections (e.g. osteosclerosis in otters, pachy-osteosclerosis in manatees) compared to terrestrial taxa (e.g. bovids, horses, Gray et al. 2007). The ribs of *Indohyus* display an osteosclerotic medullary cavity caused by an increase in cortical dimensions, whereas archaeocetes evolved osteosclerosis by only slightly increasing the cortical thickness, but greatly thickening the trabecular struts within the medullary cavity (Gray et al. 2007; Madar 2007).

Vertebral cross-sectional dimensions are poorly studied. Madar (2007) noted a thick cortical layer to the vertebra of the pakicetid *Ichthyolestes*. A CT scan through the midshaft of a caudal vertebra (RR 249) indicated that *Indohyus* had a thin cortical layer, but the centre of the vertebra was filled with bone, presumably in the form of trabecular struts (Figure 7.13).

Phylogenetic analyses show that *Indohyus* is most consistently the sister taxon of cetaceans (Thewissen et al. 2007; Geisler and Theodor 2009; Spaulding et al. 2009) and this analysis of its postcranial skeleton indicates that *Indohyus* is a morphological intermediate between primitive terrestrial artiodactyls (i.e. *Diacodexis* and *Gujaratia*) and the earliest cetaceans. Diacodexids, *Indohyus* and pakicetids display skeletal morphologies consistent with adaptations associated with cursoriality (Rose 1985; Madar 2007). The skeletons of pakicetids are derived in their robust skeletal elements and the presence of osteosclerosis within the skeleton. In contrast, *Indohyus* retains the gracile skeleton of primitive artiodactyls, but also displays osteological correlates of robust axial musculature and a hyperostotic appendicular skeleton to a lesser degree than seen in pakicetids.

Skeletal evolution along the initial phase of the land-to-sea transition

By placing *Indohyus* in phylogenetic context, it is possible to reconstruct the sequence of skeletal evolution that artiodactyls and cetaceans followed to become aquatic. Modern and fossil terrestrial artiodactyls lack hyperostosis in the postcranial skeleton, typically hold their head well above the vertebral column during aquatic locomotion and utilise quadrupedal paddling for aquatic propulsion. *Indohyus* represents a critical intermediate between

Table 2. Cortical bone thickness in the long bones of artiodactyls.

Taxon	Specimen ID	Bone	Medullary Cavity as % Bone Diamater	Reference
Indohyus sp.†	RR 157	Humerus	48	Thewissen et al. (2007)
Ichthyolestes pinfoldi †	H-GSP 96227, 96247	Humerus	14-15	Thewissen et al. (2007)
Andrewsiphius sloani †	IITR-2871	Humerus	41	Thewissen et al. (2007)
Marmota sp.	HT	Humerus	56	Thewissen et al. (2007)
Cainotherium sp.†	IVAU unnumbered	Humerus	58	Thewissen et al. (2007)
Merycoidodon sp.†	USNM 2459	Humerus	61	Thewissen et al. (2007)
Oreotragus sp.	USNM 314959	Humerus	63	Thewissen et al. (2007)
Sus barbatus	USNM 34891	Humerus	93	Thewissen et al. (2007)
Hyemoschus aquaticus	CMNH 17918	Humerus	68	this study
Tragulus javanicus	CMNH 17917	Humerus	67	this study
Tragulus javanicus	CMNH 28126	Humerus	57	this study
Indohyus sp.†	RR 42	Femur	42	Thewissen et al. (2007)
Ichthyolestes pinfoldi †	H-GSP 30345	Femur	25	Thewissen et al. (2007)
Nalacetus ratimitus †	H-GSP 98124	Femur	54	Thewissen et al. (2007)
Ambulocetus natans †	H-GSP 18507	Femur	57	Thewissen et al. (2007)
Hippopotamus amphibious	USNM 162977	Femur	55	Thewissen et al. (2007)
Cainotherium sp.†	IVAU unnumbered	Femur	60	Thewissen et al. (2007)
Merycoidodon sp.†	USNM 2460	Femur	68	Thewissen et al. (2007)
Hyemoschus aquaticus	CMNH 17918	Femur	78	this study
Sus barbatus	USNM 34891	Femur	70	Thewissen et al. (2007)
Tragulus javanicus	USNM 578462	Femur	63	Thewissen et al. (2007)
Tragulus javanicus	CMNH 17917	Femur	71	this study
Tragulus javanicus	CMNH 28126	Femur	67	this study
Leptomeryx sp.†	USNM 362713	Femur	64	Thewissen et al. (2007)
Saiga sp.	USNM 336264	Femur	68	Thewissen et al. (2007)
Capra hircus	CMNH B640	Femur	70	this study
Indohyus sp.†	RR 46	Tibia	39	this study
Hyemoschus aquaticus	CMNH 17918	Tibia	68	this study
Tragulus javanicus	CMNH 17917	Tibia	60	this study
Tragulus javanicus	CMNH 28126	Tibia	61	this study
Capra hircus	CMNH B640	Tibia	51	this study
Indohyus sp.†	RR 225	Metatarsal	50	this study
Hyemoschus aquaticus	CMNH 17918	Metatarsal	58	this study
Tragulus javanicus	CMNH 17917	Metatarsal	62	this study
Tragulus javanicus	CMNH 28126	Metatarsal	62	this study
Capra hircus	CMNH B640	Metatarsal	59	this study
Indohyus sp.†	RR 228	Metacarpal	57	this study
Indohyus sp.†	RR 271	Metacarpal	55	this study
Hyemoschus aquaticus	CMNH 17918	Metacarpal	55	this study
Tragulus javanicus	CMNH 17917	Metacarpal	43	this study
Tragulus javanicus	CMNH 28126	Metacarpal	36	this study
Indohyus sp.†	RR 235	Rib	62	this study
Indohyus sp.†	RR 217	Rib	59	this study
Hyemoschus aquaticus	CMNH 17918	Rib	58	this study

Percentage of the medullary cavity diameter to total bone diameter in skeletal elements of fossil and extant artiodactyls, and a large rodent. †indicates a fossil taxon.

terrestrial artiodactyls and semi-aquatic pakicetids, as *Indohyus* displayed incipient osteosclerosis in some postcranial elements, probably held its head well above the vertebral column during aquatic locomotion and utilised quadrupedal paddling to propel itself through the water while the tail probably acted to stabilise the animal. The metapodials of *Indohyus* are only slightly longer than those of known terrestrial taxa.

In comparison, pakicetids displayed intense and systemic osteosclerosis throughout the postcranial skeleton, and during aquatic locomotion probably held their heads parallel to the vertebral column like crocodilians, and utilised a combination of pelvic paddling and caudal undulations for aquatic propulsion as in modern lutrines (Madar 2007). Pakicetids also displayed long metapodial elements, which perhaps could have been joined by interdigital webbing that increased the pedal surface area during soft substrate and aquatic locomotion (Madar 2007).

These data indicate that osteosclerosis and metapodial elongation were the first morphological characteristics of the artiodactyl postcranial skeleton to change along the

land-to-sea transition. Only incipient cortical bone osteosclerosis is present in *Indohyus*, but the greatest cortical bone thickness in Cetacea is documented in pakicetids (Madar 2007). Later diverging archaeocetes (e.g. ambulocetids, remingtonocetids, protocetids and basilosaurids) employed only slight cortical bone thickening, but decreased medullary cavity area by increasing the thickness of trabecular struts within this cavity (Gray et al. 2007; Madar 2007). The skeletons of modern cetaceans are lightened, or osteoporotic, due to a decrease in bone volume and/or density, usually within the ribs and appendicular skeleton (Felts and Spurrell 1965, 1966; De Buffrénil et al. 1985, 1986; De Buffrénil and Schoevaert 1988; de Ricqlès and De Buffrénil 2001; Butti et al. 2007). Cortical bone osteosclerosis in *Indohyus* and pakicetids was probably a key morphological feature that facilitated the initial artiodactyl and subsequent cetacean invasion of the Eocene seas by counteracting buoyancy and aiding foraging at depth.

Indohyus only displays incipient metapodial elongation. The metapodials are longer in pakicetids, and the metatarsals of *Ambulocetus* are the longest in Cetacea. Later diverging archaeocetes (e.g., remingtonocetids and protocetids) also display long metatarsals, but reduction in the hindlimb in basilosaurids and later diverging taxa facilitated a streamlined body contour for aquatic locomotion. The elongation of metapodials in early archaeocetes probably acted to increase the pedal surface area initially for locomotion in soft substrates, such as muds along bodies of water, and this webbing also likely facilitated the aquatic locomotion. The substrates that these early archaeocetes and their closest relatives (raoellids) encountered during locomotion are well understood, thanks to a sedimentological study (Aslan and Thewissen 1996) indicating the earliest cetaceans (pakicetids) and their closest fossil artiodactyl relatives (raoellids) lived in shallow freshwater bodies that had an abundance of mud (Aslan and Thewissen 1996; Thewissen et al. 2007).

Thewissen et al. (2007) proposed a potential evolutionary scenario for the origin of cetaceans in which their terrestrial artiodactyl (even-toed ungulate) ancestors took to the water initially for shelter from predators (similar to some extant tragulids, Dubost 1978; Meijaard et al. 2010). From this initial wading step, early cetacean lineages spent successively more time in water similar to modern day *Hippopotamus* (Sheppe and Osborne 1971; Gray et al. 2007; Madar 2007) and eventually began feeding in water. This model predicts that the raoellids and the earliest cetaceans were able to wade and swim effectively, and osteosclerosis and metapodial elongation may have facilitated the earliest parts of the land-to-sea transition.

Acknowledgements

We thank Drs Brian L. Beatty and M.D. Uhen for their thoughtful reviews, and Drs T.L. Hieronymus, C. Vinyard, W.E. Horton, Jr, J. Wenstrup, and R.B. Cooper for additional comments on this manuscript. We thank the late F. Obergfell for allowing us to prepare sediment blocks containing fossils of *Indohyus* that were originally collected by A. Ranga Rao; A. Maas, R.W. Conley, J. Sensor and B.J. Schneider for preparation; S. Usip and R.W. Conley, M. Colbert and UTCT staff for high resolution CT scans. This research was funded by the National Science Foundation (NSF-EAR 0745543 to J.G.M. Thewissen), and the Skeletal Biology Research Focus Area of Northeastern Ohio Universities College of Medicine. S. Bajpai would like to thank the Department of Science & Technology, Government of India for financial support.

Notes

1. Email: thewisse@neoucom.edu
2. Email: sunilfes@iitr.ernet.in
3. Email: bntiwari@wihg.res.in

References

Aslan A, Thewissen JGM. 1996. In: Godinot M, Gingerich PD, editors. Preliminary evaluation of paleosols and implications for interpreting vertebrate fossil assemblages, Kuldana Formation, northern Pakistan. Montpellier: Palaeovertebrata. p. 261–277. 25(2–4).

Bajpai S, Gingerich PD. 1998. New early Eocene cetacean from India and the timing of the origin of whales. Prod Natl Acad Sci USA. 95:15464–15468.

Bajpai S, Thewissen JGM. 2000. A new, diminutive whale from Kachchh (Gujarat, India) and its implications for locomotor evolution of cetaceans. Curr Sci. 79:1478–1482.

Bajpai S, Kapur VV, Das DP, Tiwari BN, Saravanan N, Sharma R. 2005. Early Eocene land mammals from Vastan lignite mine, District Surat (Gujarat), Western India. J Paleontol Soc India. 50:101–113.

Beatty BL, Dooley AC. 2009. Injuries in a mysticete skeleton from the Miocene of Virginia, with a discussion of buoyancy and the primitive feeding mode in the Chaeomysticeti, Jeffersoniana. Contrib Virginia Mus Nat Hist. 20:1–28.

Behrensmeyer AK, Deino AL, Hill A, Kingston JD, Saunders JJ. 2002. Geology and geochronology of the middle Miocene Kipsaramon site complex, Muruyur Beds, Tugen Hills, Kenya. J Hum Evol. 42:11–38.

Boisserie J, Lihoreau RF, Brunet M. 2005a. Origins of Hippopotamidae (Mammalia, Cetartiodactyla): towards resolution. Zool Scr. 34:119–143.

Boisserie J, Lihoreau RF, Brunet M. 2005b. The position of Hippopotamidae within Cetartiodactyla. Proc Natl Acad Sci USA. 102(5):1537–1541.

Buchholtz EA. 1998. Implications of vertebral morphology for locomotor evolution in early Cetacea. In: Thewissen JGM, editor. The Emergence of Whales: evolutionary Patterns in the Origin of Cetacea. New York: Plenum Press. p. 325–351.

De Buffrénil V, Schoevaert D. 1988. On how the periosteal bone of the delphinid humerus becomes cancellous: ontogeny of a histological specialization. J Morphol. 198:149–164.

De Buffrénil V, Collet A, Pascal M. 1985. Ontogenetic development of skeletal weight in a small delphinid, Delphinus delphis (Cetacea: Odontoceti). Zoomorphology. 105:336–344.

De Buffrénil V, De Sire JY, Schoevaert D. 1986. Comparison de la structure et du volume squelettiques entre un delphinidé (*Delphinus delphis* L.) et un mammifère terrestre (*Panthera* leo L.). Can J Zool. 64:1750–1756.

De Buffrénil V, De Ricqlès A, Ray CE, Domning DP. 1990. Bone histology of the ribs of thearchaeocetes (Mammalia: Cetacea). J Vert Paleontol. 10:455–466.

De Buffrénil V, Astibia H, Pereda Suberbiola X, Berreteaga A, Bardet N. 2008. Variation in bone histology of middle Eocene sirenians from Western Europe. Geodiversitas. 30(2):425–432.

Butti C, Corain L, Cozzi B, Podestà M, Pirone A, Affronte M, Zotti A. 2007. Age estimation in the Mediterranean bottlenose dolphin

Tursiops truncatus (Montagu 1821) by bone density of thoracic limb. J Anat. 211:639–646.
Clementz MT, Goswami A, Gingerich PD, Koch PL. 2006. Isotopic records from early whales and sea cows: contrasting patterns of ecological transition. J Vert Paleontol. 26(2):355–370.
Cooper LN. 2009. Forelimb anatomy. In: Perrin WF, Würsig B, Thewissen JGM, editors. Encyclopedia of Marine Mammals. 2nd ed.San Diego: Elsevier. p. 449–452.
Cooper LN, Thewissen JGM. 2010. In press. Indohyus and the origin of whales. 2010 Yearbook of Science and Technology.
Cooper LN, Dawson SD, Reidenberg JS, Berta A. 2007. Neuromuscular anatomy and evolution of the cetacean forelimb. Anat Record Adv Integr Anat Evol Biol. 209(9):1121–1137.
Cooper LN, Sedano N, Johannson S, May B, Brown J, Holliday CM, Fish FE. 2008. Hydrodynamic performance of the minke whale (*Balaenoptera acutorostrata*) flipper. J Exp Biol. 211:1859–1867.
Dehm R, zu Oettingen-Spielberg T. 1958. Paläontologische und geologische Untersuchungen im Tertiär von Pakistan. 2. Die mitteleocänen Säugetiere von Ganda Kas bei Basal in Nordwest-Pakistan. Bayerische Akademie der Wissenschaften, Mathematisch-Naturwissenschaftliche Klasse. Abhandlungen Neue Folge Heft. 91:1 − 54.
Domning DP, De Buffrénil V. 1991. Hydrostasis in the sirenia: quantitative data and functional interpretations. Mar Mammal Sci. 7:331–368.
Domning DP, Myrick AC, Jr. 1980. Tetracycline marking and the possible layering rate of bone in an Amazonian manatee (*Trichechus inunguis*). In: Perrin WF, Myrick AC, Jr., editors. Age determination of toothed whales and sirenians. Special Issue 3, Reports of the International Whaling Commission. Cambridge: International Whaling Commission. p. 203.
Dubost G. 1978. Un apercu sur l'écologie du chevrotain africain *Hyemoschus aquaticus* Ogilby, Artiodactyle Tragulide. Mammalia. 42:1–62.
Endo H, Sasaki M, Kimura J, Fukuta K. 2006. Functional strategies of the hindlimb muscles in the mouse deer. Mammal Study. 31:73–78.
English AWM. 1976. Functional anatomy of the hands of fur seals and sea lions. Am J Anat. 147:1–17.
English AWM. 1977. Structural correlates of forelimb function in fur seals and sea lions. J Morphol. 151:325–352.
Fawcett DW. 1942. The amedullary bones of the Florida manatee (*Trichechus latirostris*). Am J Anat. 71:271–309.
Felts WJL, Spurrell FA. 1965. Structural orientation and density in cetacean humeri. Am J Anat. 116:171–204.
Felts WJL, Spurrell FA. 1966. Some structural and developmental characteristics of cetacean (odontocete) radii. A study of adaptive osteogenesis. Am J Anat. 118:103–134.
Fish FE, Battle JM. 1995. Hydrodynamic design of the humpback whale flipper. J Morphol. 225:51–60.
Fish FE, Stein BR. 1991. Functional correlates of differences in bone density among terrestrial and aquatic genera in the family Mustelidae (Mammalia). Zoomorphology. 110:339–345.
Fordyce RE, de Muizon C. 2001. Evolutionary history of cetaceans: a review. In: Mazin JM, de Buffrénil V, editors. Secondary Adaptation of Tetrapods to Life in Water. München, Germany: Verlag Dr Friedrich Pfeil. p. 169–233.
Geisler JH. 2001. New morphological evidence for the phylogeny of Artiodactyla, Cetacea, and Mesonychidae. Am Mus Novitates. 3344:1–53.
Geisler JH, Theodor JM. 2009. *Hippopotamus* and whale phylogeny. (E1-E4 on-line only) Nature. 458.
Geisler JH, Uhen MD. 2003. Morphological support for a close relationship between hippos and whales. J Vertebrate Paleontol. 23:991–996.
Geisler JH, Uhen MD. 2005. Phylogenetic relationships of extinct Cetartiodactyls: results of simultaneous analyses of molecular, morphological, and stratigraphic data. J Mammalian Evol. 12:145–160.
Geisler JH, Theodor JM, Uhen MD, Foss SE. 2007. Phylogenetic relationships of cetaceans to terrestrial artiodactyls. In: Prothero DR, Foss SE, editors. The evolution of artiodactyls. Baltimore: Johns Hopkins University Press. p. 19–31.
Germain D, Laurin M. 2005. Microanatomy of the radius and lifestyle in amniotes (vertebrata, tetrapoda). Zool Scr. 34:335–350.
Gingerich PD. 1977. A small collection of fossil vertebrates from the middle Eocene Kuldana and Kohat formations of Punjab (Pakistan). Contrib Mus Paleontol Univ Michigan. 24:190–203.
Gingerich PD. 1989. New earliest Wasatchian mammalian fauna from the Eocene of Northwestern Wyoming: composition and diversity in a rarely sampled high-floodplain assemblage. Univ Michigan Papers Paleontol. 28:1–97.
Gingerich PD. 2003. Land-to-sea transition in early whales: evolution of Eocene Archaeoceti (Cetacea) in relation to skeletal proportions and locomotion of living semiaquatic mammals. Paleobiology. 29:429–454.
Gingerich PD, Russell DE. 1981. Pakicetus inachus, a new archaeocete (Mammalia, Cetacea) from the early-middle Eocene Kuldana Formation of Kohat (Pakistan). Contrib Mus Paleontol Univ Michigan. 25(11):235 − 246.
Gingerich PD, Russell DE. 1990. Dentition of early Eocene Pakicetus (Mammalia, Cetacea). Contrib Mus Paleontol Univ Michigan. 28(1):1–20.
Gingerich PD, Raza SM, Arif M, Anwar M, Zhou X. 1994. New whale from the Eocene of Pakistan and the origin of cetacean swimming. Nature. 368:844–847.
Gingerich PD, Ul Haq M, Zalmout IS, Khan IH, Malkani MS. 2001. Origin of whales from early artiodactyls: hands and feet of Eocene Protocetidae from Pakistan. Science. 293:2239–2242.
Gingerich PD, Ul Haq M, Koenigswald WV, Sanders WJ, Smith HB, Zalmout IS. 2009. New protocetid whale from the middle Eocene of Pakistan: birth on land, precocial development, and sexual dimorphism. PLoS One. 4(2):1–20.
Gordon KR. 1981. Locomotor behavior of the walrus (*Odobenus*). J Zool Lond. 195:349–357.
Gray NM, Kainec K, Madar S, Tomko L, Wolfe S. 2007. Sink or swim? Bone density as a mechanism for buoyancy control in early cetaceans. Anat Record. 290:638–653.
Graur D, Higgins DG. 1994. Molecular evidence for the inclusion of cetaceans within the order Artiodactyla. Mol Biol Evol. 11:357–364.
Gunnell GF, Bartels WS. 2001. Basin margins, biodiversity, evolutionary innovation, and the origin of new taxa. In: Gunnell GF, editor. Eocene biodiversity: unusual occurrences and rarely sampled habitats. New York: Kluwer Academic/Plenum Publishers. p. 404–430.
Hartman DS. 1979. Ecology and behavior of the manatee (*Trichechus manatus*). Amrican Society of Mammalogists, Special Publication No. 5.
Houssaye A. 2009. 'Pachyostosis' in aquatic amniotes: a review. Integr Zool. 4:325–340.
Hulbert RC. 1998. Postcranial osteology of the North American middle Eocene protocetid Georgiacetus. In: Thewissen JGM, editor. Emergence of whales: evolutionary patterns in the origin of cetacea. New York: Plenum Press. p. 235–267.
Hulbert RC, Petkewich RM, Bishop GA, Bukry D, Aleshire DP. 1998. A new middle Eocene protocetid whale (Mammalia: Cetacea: Archaeoceti) and associated biota from Georgia. J Paleontol. 72:905–925.
Kaiser HE. 1960. Untersuchungen zur vergleichenden osteologie der fossilen und rezenten pachyostosen. Palaeontographica A. 114:113–196.
Kriloff A, Germain D, Canoville A, Vincent P, Sache M, Laurin M. 2008. Evolution of bone microanatomy of the tetrapod tibia and its use in palaeobiological inference. J Evol Biol. 21:807–826.
Krishtalka L, Stucky RK. 1985. Revision of the Wind River faunas, early Eocene of Central Wyoming. Part 7. Revision of *Diacodexis* (Mammalia, Artiodactlya). Annals of Carnegie Museum. Carnegie Mus Nat Hist. 54(14):413–486.
Krishtalka L, Stucky RK. 1986. Early Eocene artiodactyls from the San Juan Basin, New Mexico, and the Piceance Basin, Colorado. Contributions to Geology, University of Wyoming, Special Paper. 3:183–196.
Kumar K, Sahni A. 1985. Eocene mammals from the Upper Subathu Group, Kashmir Himalaya, India. J Vertebrate Paleontol. 5(2):153–168.

Ling JK. 1974. The integument of marine mammals. In: Harrison R.J., editor. Functional anatomy of marine mammals. London: Academic Press. p. 1–44.
Liu FGR, MiyamOTO MM. 1999. Phylogenetic assessment of molecular and morphological data for eutherian mammals. Syst Biol. 48:54–64.
Lum JK, Nikaido M, Shimamura M, Shimodaira H, Shedlock AM, Okada N, Hasegawa M. 2000. Consistency of SINE insertion topology and flanking sequence tree: quantifying relationships among Cetartiodactyls. Mol Biol Evol. 17:1417–1424.
Madar SI. 1998. Structural adaptations of early archaeocete long bones. In: Thewissen JGM, editor. The emergence of whales. New York: Plenum Press. p. 353–378.
Madar SI. 2007. The postcranial skeleton of early Eocene pakicetid cetaceans. J Paleontol. 81:176–200.
Madar SI, Thewissen JGM, Hussain ST. 2002. Additional holotype remains of *Ambulocetus natans* (Cetacea, Ambulocetidae), and their implications for locomotion in early whales. J Vertebrate Paleontol. 22(2):405–422.
Marcot JD. 2007. Molecular phylogeny of terrestrial artiodactyls: conflicts and resolution. In: Prothero DR, Foss SE, editors. The evolution of artiodactyls. Baltimore: Johns Hopkins University Press. p. 4–18.
Meijaard E, de Umilaela G, Wijeyeratne S. 2010. Aquatic escape behavior in mouse-deer provides insight into tragulid evolution. Mammalian Biol. 75:471–473.
Montgelard C, Catzeflis FM, Douzery E. 1997. Phylogenetic relationships of artiodactyls and cetaceans as deduced from the comparison of cytochrome b and 12S rRNA mitochondrial sequences. Mol Biol Evol. 14:500–559.
Nowak RM. 1991. Walker's mammals of the World. 5th ed. Vol. II. Baltimore: John's Hopkins University Press. p. 1629.
O'Leary MA. 1998. Phylogenetic and morphometric reassessment of the dental evidence for a mesonychian and cetacean clade. In: Thewissen JGM, editor. The emergence of whales. Plenum Press: New York. p. 133–161.
O'Leary MA, Gatesy J. 2008. Impact of increased character sampling on the phylogeny of Cetartiodactyla (Mammalia): combined analysis including fossils. Cladistics. 24(4):397–442.
Pickford M. 1983. On the origins of Hippopotamidae together with descriptions of two species, a new genus and a new submfamily from the Miocene of Kenya. Géobios. 16:193–217.
Pilgrim GE. 1940. Middle Eocene mammals from north-west India. Proc Zool Soc Lond Ser B. 110:127–152.
Price SA, Bininda-Edmonds ORP, Gitttleman JLA. 2005. complete phylogeny of the whales, dolphins, and even-toed hoofed mammals (Cetartiodactyla). Biol Rev. 80:445–473.
Ranga Rao A. 1971. New mammals from Murree (Kalakot zone) of the Himalayan foot hills near Kalakot, Jammu and Kashmir State, India. J Geol Soc India. 12(2):125–134.
Ranga Rao A, Misra VN. 1981. On the new Eocene mammal localities in the Himalayan foot-hills. Himalayan Geol. 11:422–428.
Ridgway SH, Howard R. 1979. Dolphin lung collapse and intramuscular circulation during free diving: evidence from nitrogen washout. Science. 206:1182–1183.
de Ricqlès, De Buffrénil V. 2001. Bone histology, heterochronies, and the return of tetrapods to life in water: where are we? In: Mazin JM, de Buffrénil V, editors. Secondary adaptation of tetrapods to life in water. München: Verlag. p. 289–310.
Roe LJ, Thewissen JGM, Quade J, O'Neil JR, Bajpai S, Sahni A, Hussain ST. 1998. Isotopic approaches to understanding the terrestrial-to-marine transition of the earliest cetaceans. In: Thewissen JGM, editor. The Emergence of Whales. New York: Plenum Press. p. 399–442.
Rose KD. 1985. Comparative osteology of North American dichobunid artiodactyls. J Paleontol. 59(5):1203–1226.
Russell DE, Zhai RJ. 1987. The Paleogene of Asia: mammals and stratigraphy. Serie C, Sciences de la Terre Mémoires du Muséum National D'Histoire Naturelle. 52. 488 p.
Sahni A, Khare SK. 1971. Three new Eocene mammals from Rajauri District, Jammu and Kashmir. J Palaeontol Soc India. 16:41–53.
Sahni A, Bhatia SB, Hartenberger JL, Jaeger JJ, Kumar K, Sudre J, Vianey-Liaud M. 1981. Vertebrates from the Subathu Formation and comments on the biogeography of Indian subcontinent during the early Paleogene. Bull Soc Géol France XXIII. 6:689–695.
Schaeffer B. 1947. Notes on the origin and function of the artiodactyl tarsus. Am Mus Novitates. 1356:1–24.
Shedlock AM, Milinkovitch MC, Okada N. 2000. SINE evolution, missing data and the origin of whales. Sys Biol. 49:808–817.
Sheppe W, Osborne T. 1971. Patterns of use of a flood plain by Zambian mammals. Ecol Monogr. 41(3):179–205.
Spaulding M, O'Leary MA, Gatesy J. 2009. Relationships of Cetacea (Artiodactyla) among mammals: Increased taxon sampling alters interpretations of key fossils and character evolution. PLos One. 4(9):e7062.
Sudre J, Russell DE, Louis P, Savage DE. 1983. Les artiodactyles de l'Éocène inférieur d'Europe. Bulletin de la Musee d'Histoire Naturelle de Paris. 5(3):281–333.
Tarassof FJ. 1972. Comparative aspects of the hind limbs of the river otter, sea otter, and seals. In: Harrison RJ, editor. Functional anatomy of marine mammals. Vol 1. Plenum Press: New York. p. 333–359.
Taylor MA. 1993. Stomach stones for feeding or buoyancy? The occurrence and function of gastroliths in marine tetrapods. Philos Trans R Soc Lond B. 341:163–175.
Taylor MA. 2000. Functional significance of bone ballastin in the evolution of buoyancy control strategies by aquatic tetrapods. Hist Biol. 14:15–31.
Theodor JM, Foss SE. 2005. Deciduous dentitions of Eocene cebochoerid artiodactyls and cetartiodactyl relationships. J Mammalian Evol. 12:161–181.
Theodor JM, Erfurt J, Métais G. 2007. The earliest artiodactyls: Diacodexeidae, Dichobunidae, Homacodontidae, Leptochoeridae, and Raoellidae. In: Prothero DR, Foss SE, editors. The evolution of artiodactyls. Baltimore: Johns Hopkins University Press. p. 32–58.
Thewissen JGM, Bajpai S. 2009. New skeletal material of *Andrewsiphius and Kutchicetus*, two Eocene cetaceans from India. J Paleontol. 83(5):635–663.
Thewissen JGM, Fish FE. 1997. Locomotor evolution in the earliest cetaceans: functional model, modern analogues, and paleontological evidence. Paleobiology. 23(4):482–490.
Thewissen JGM, Hussain ST. 1990. Postcranial osteology of the most primitive artiodactyl *Diacodexis pakistanensis* (Dichobunidae). Anatomia Histologia Embryologia. 19:37–48.
Thewissen JGM, Hussain ST. 1998. Systematic review of the Pakicetidae, early and middle Eocene Cetacea (Mammalia) from Pakistan and India. In: Beard KC, Dawson MR, editors. Dawn of the age of mammals in Asia. Bulletin of Carnegie Museum of Natural History 34. p. 220–238.
Thewissen JGM, Madar SI. 1999. Ankle morphology of the earliest cetaceans and its implications for the phylogenetic relations among ungulates. Syst Biol. 48(1):21–30.
Thewissen JGM, Russell DE, Gingerich PD, Hussain ST. 1983. A new dichobunid artiodactyl (Mammalia) from the Eocene of North-West Pakistan. Part I: Dentition and classification. Proceedings of the Koninklike Nederlandse Akademie Van Wetenschapen, Serie B. 86:153–180.
Thewissen JGM, Gingerich PD, Russell DE. 1987. Artiodactyla and perissodactyla (Mammalia) From the early-middle Eocene Kuldana Formation of Kohat (Pakistan). Contrib Mus Paleontol Univ Michigan. 27(10):247–274.
Thewissen JGM, Hussain ST, Arif M. 1994. Fossil evidence for the origin of aquatic locomotion in archaeocete whales. Science. 263:210–212.
Thewissen JGM, Madar SI, Hussain ST. 1996. *Ambulocetus natans*, an Eocene cetacean (Mammalia) from Pakistan, Courier Forschungsinstitut Senckenberg 191. Frankfurt AM. 28(6):1–86.
Thewissen JGM, Williams EM, Hussain ST. 2001a. Eocene mammal faunas from northern Indo-Pakistan. J Vertebrate Paleontol. 21(2):347–366.
Thewissen JGM, Williams EM, Roe LJ, Hussain ST. 2001b. Skeletons of terrestrial cetaceans and the relationships of whales to artiodactyls. Nature. 413:277–281.
Thewissen JGM, Cohn MJ, Stevens LS, Bajpai S, Heyning J, Horton WE, Jr. 2006. Developmental basis for hind-limb loss in dolphins and origin of the cetacean body plan. Proc Natl Acad Sci. 103:8414–8418.

Thewissen JGM, Cooper LN, Clementz MT, Bajpai S, Tiwari BN. 2007. Whales originated from artiodactyls in the Eocene epoch of India. Nature. 450:1190–1194.

Thewissen JGM, Cooper LN, George C, Bajpai S. 2009. From land to water: the origin of whales, dolphins and porpoises. Evol Educ Outreach. 2:272–288.

Uhen MD. 2004. Form, function and anatomy of Dorudon atrox (Mammalia, Cetacea): an archaeocete from Middle to Late Eocene of Egypt. Univ Michigan Papers Paleontol. 34:1–222.

Wall WP. 1983. The correlation between high limb-bone density and aquatic habits in recent mammals. J Paleontol. 57(2):197–207.

Weber PW, Howle LW, Murray MM, Fish FE. 2009. Lift and drag performance of odontocete flippers. J Exp Biol. 212(14):2149–2158.

West RM. 1980. Middle Eocene large mammal assemblage with Tethyan affinities, Ganda Kas region, Pakistan. J Paleontol. 54(3):508–533.

Wings O. 2007. A review of gastrolith function with implications for fossil vertebrates and a revised classification. Acta Palaentol Polonica. 52(1):1–16.

Appendix

Catalogue of *Indohyus* postcranial elements from the A. Ranga Rao collection used in this analysis.

Specimen number	Skeletal material
Ribs	
RR 168	Rib, cranial, crushed, lacks distal end
RR 217	Three fragments of rib shaft, lacks head, neck and end
RR 221	Rib shaft, crushed, lacks proximal and distal ends
RR 222	Rib shaft, crushed, lacks proximal and distal ends
RR 235	Two fragments of rib shaft, lacks proximal and distal ends
RR 243	Rib, cranial, with head, neck and partial shaft, lacks distal end
RR 244	Rib, crushed head and shaft, lacks distal end
RR 245	Rib shaft, crushed, lacks proximal and distal ends
RR 305	Rib, lacks proximal and distal ends
Vertebrae	
RR 7	Two articulated vertebrae, lacks ventral half of each vertebra, and body of smallest vertebra
RR 220	Vertebra, dorsoventrally crushed, lacks caudal articular facet, caudal portion of body
RR 338	Vertebra, fragment, lacks processes, sheared
Cervical Vertebrae	
RR 198	Cervical vertebra, crushed, lacks spinous process, cranial facets, tips of transverse processes
RR 335	Cervical vertebra, crush along dorsoventral axis, lacks caudal articular facets and scalene processes
RR 86	Atlas, lacks transverse processes, lacks part of left articular facet for axis
RR 165	Atlas, right transverse process missing most of its cranial portion, dorsal arch lacks its cranial surface and dorsal portion of occipital condyle facet
RR 33	Cervical vertebra 3, lacks all but base of spinous process, left transverse foramen, cranial and caudal surface of vertebral body
RR 342	Cervical vertebra 4, broken spinous and transverse processes, and cranial facets
RR 38	Cervical vertebra 5, lacks tip of spinous process, articular facets on left side
RR 136	Cervical vertebra 5, lacks spinous process, distal half of right transverse process, cranial epiphysis
RR 332	Cervical vertebra 5, all processes on left surface broken, spinous process broken, sheared; fused to shaft of a radius that lacks its proximal half
RR 337	Cervical vertebra 5, smashed, processes broken
RR 195	Cervical vertebra 7, lacks cranial half of bone, tips of transverse processes, left caudal facet
Cranial Thoracic Vertebrae	
RR 20	Cranial thoracic vertebra, crushed, lacks cranial facets, transverse processes and had unfused epiphyses
RR 21	Cranial thoracic vertebra, crushed, spinous process lacks tip, transverse processes lack tips
RR 247	Cranial thoracic vertebra, cranial and caudal surface of body incomplete, lacks spinous process Middle Thoracic Vertebrae
RR 85	Middle thoracic vertebra, unfused cranial epiphysis and lacks cranial articular facets
RR 137	Middle thoracic vertebra, crushed, spinous process lacks tip, cranial articular surfaces broken tips, deformed body lacks part of caudal face
RR 242	Middle thoracic vertebra, crushed, spinous process lacks tip, broken right transverse process and caudal articular surfaces
RR 292	Middle thoracic vertebra, lacks tip of spinous process, transverse processes and ventral half of body, dorsal half of body is crushed
Terminal Thoracic Vertebrae	
RR 25	Thoracic vertebra, tentatively identified as T13, crushed mediolaterally axis, tips of cranial articular facets, transverse processes, left accessory process, left cranial costal fovea
RR 239	Two articulated caudal thoracic vertebra articulated with L1, crushed mediolaterally, spinous process broken, lacks ventral surface of each vertebra (see also description in 'Lumbar Vertebrae')
RR 344	Thoracic vertebrae, two fused along centra, dorsoventrally crushed, processes broken
Lumbar Vertebrae	
RR 215	Lumbar vertebra, lacks right transverse process and cranial half of vertebra
RR 218	Body of a lumbar vertebra, lacks all processes, cranial and caudal epiphyses unfused
RR 219	Lumbar vertebra, middle, dorsoventrally crushed, lacks spinous and transverse processes
RR 239	Lumbar vertebra, cranial, in articulation with two caudal thoracic vertebrae, lacks tip of spinous process, ventral surface of vertebra (see also description in 'Terminal Thoracic Vertebrae')
RR 296	Lumbar vertebrae, two attached, but not articulated, mediolaterally crushed, lack tips of spinous processes and transverse processes, smallest vertebra lacks caudal articular facets
RR 343	Lumbar vertebra, lacks ventral half of body, broken tips of caudal processes

Appendix – *continued*

Specimen number	Skeletal material
Sacrum	
RR 156	Sacral vertebrae S1-S3, fused, cannot determine if S4 is also fused. S1 with complete body, lacks spinous and transverse processes, and the left auricular surface. S2, S3 lacks tips of left transverse processes, right surface of median sacral crest, right intermediate sacral crest
Caudal Vertebrae	
RR 45	Caudal vertebra, middle, lacks left mammillary process, left cranial transverse process, caudal transverse processes,and ventrolateral surfaces of caudal aspect of vertebra
RR 65	Caudal vertebra, terminal, with body dorsoventrally crushed, lacks left cranial transverse process
RR 75	Caudal vertebra, middle, lacks some transverse processes
RR 169	Caudal vertebra, dorsoventrally crushed, lacks right cranial articular process, left caudal articular processes
RR 184	Caudal vertebra, middle, mediolaterally crushed, lacks distal half
RR 249	Caudal vertebra, terminal, lacks left cranial transverse process
RR 294	Caudal vertebra, asymmetrical, crushed right cranial transverse and transverse processes, lacks tip of caudal articular processes
RR 304	Caudal vertebra, crushed, lacks cranial articular processes
RR 339	Caudal vertebra, sheared, broken right cranial and caudal articular facets, and transverse processes
RR 341	Caudal vertebra, fragment, lacks processes and cranial half and lateral portion of body
Scapula	
RR 131	Scapula, left, lacks cranial and dorsal aspects
RR 171	Scapula fragment, right, distal aspect of blade, spine and coracoid process
RR 263	Glenoid fossa
Humerus	
RR 145	Humerus, left
RR 149	Humerus, left
RR 31	Humerus, right, lacks distal half
RR 90	Humerus, fragmentary proximal epiphysis
RR 140	Humerus, lacks distal half
RR 157	Humerus, left, lacks distal half
RR 316	Humerus, distal half, lacks proximal half, crushed in mediolateral plane
RR 318	Humerus, head, greater and lesser trochanters
Radius	
RR 2	Radius, two shaft fragments, lacks proximal epiphysis
RR 36	Radius, fragment of distal shaft, epiphysis
RR 79	Radius, shaft lacks proximal epiphysis, crushed distal epiphysis
RR 122	Radius, proximal epiphysis
RR 265	Radius, right, lacks proximal aspect of bone
RR 332	Radius, shaft, lacks proximal aspect of bone; fused to cervical vertebra 5
RR 336	Radius, lacks proximal aspect of bone
Ulna	
RR 39	Ulna, left, adult, crushed shaft and proximal epiphysis, lacks distal epiphysis
RR 142	Ulna, crushed shaft and proximal epiphysis, lacks anconeal and coracoid processes and distal epiphysis
RR 144	Ulna, right, adult, crushed shaft and proximal epiphysis, lacks olecranon process and distal epiphysis
Carpals	
RR 48	Carpal?
RR 241	Carpal?
RR 250	Magnum
Metapodial	
RR 78	Metapodial, crushed, lacks proximal half
Metacarpals	
RR 10	Metacarpal, central
RR 69	Metacarpal, distal, shaft with head, crushed in mediolateral aspect
RR 83	Metacarpal, sheared with offset shaft, proximal epiphysis crushed
RR 120	Metacarpal, central, crushed, lacks proximal half
RR 166	Metacarpal, lacks proximal half and palmar half of distal epiphysis

Appendix – *continued*

Specimen number	Skeletal material
RR 174	Metacarpal, peripheral, lacks proximal half
RR 183	Metacarpal, central, lacks distal half
RR 278	Metacarpal, central, lacks proximal epiphysis
RR 279	Metacarpal, mediolaterally crushed, lacks proximal half
RR 303	Metacarpal, lacks proximal half
RR 227	Metacarpal I, lacks palmar half and part of proximal epiphysis
RR 297	Metacarpal I, proximal shaft missing pieces of cortex, shaft broken at steep angle
RR 138	Metacarpal III, left, proximal epiphysis crushed
RR 228	Metacarpal III, left
RR 271	Metacarpal III, left
RR 270	Metacarpal IV, left, proximal shaft missing pieces of cortex
Phalanges of the Manus	
RR 3	Phalanx, proximal, central, proximal epiphysis only
RR 51	Phalanx, proximal, central, lacks distal half
RR 87	Phalanx, proximal, lacks distal half
RR 112	Phalanx, proximal, lacks proximal half
RR 113	Phalanx, proximal, central, lacks proximal half
RR 115	Phalanx, proximal, peripheral, lacks distal half
RR 117	Phalanx, proximal, peripheral, lacks part of distal epiphysis
RR 180	Phalanx, proximal, peripheral, lacks pieces of both epiphyses
RR 272	Phalanx, proximal, central, lacks distal half
RR 273	Phalanx, proximal, central
RR 274	Phalanx, proximal, central
RR 281	Phalanx, proximal, central
RR 346	Phalanx, proximal, lacks distal part of epiphysis
RR 99	Phalanx, intermediate, lacks distal epiphysis, crushed along dorsoventral plane
RR 117	Phalanx, intermediate, lacks distal epiphysis
RR 179	Phalanx, intermediate, lacks proximal epiphysis
RR 233	Phalanx, intermediate of digit I, lacks proximal epiphysis
RR 234	Phalanx, intermediate, digit I
RR 308	Phalanx, intermediate, digit I
RR 345	Phalanx, intermediate, peripheral
Pelvis	
RR 43	Innominate, left, broken ischium and pubis, lacks tip of ilium
RR 44	Innominate, left, missing iliac blade, caudal aspect of the pubis and ischium
RR 146	Acetabulum
RR 162	Acetabulum, left, fragmentary ilium, ischium
RR 187	Innominate fragment
RR 256	Innominate, right, lacks tip of ilium and pubis
RR 257	Innominate, right
RR 258	Ilium, fragment, left, partial acetabulum
RR 259	Ilium, left, lacks tip of iliac blade, pubis and caudal aspect of ishium
Femur	
RR 5	Femur, juvenile, distal shaft lacks epiphysis
RR 41	Femur, adult, left, head, proximal half of shaft, lacks trochanters
RR 42	Femur, right, adult, proximal epiphysis, proximal half of shaft
RR 89	Femur, right, adult, epiphysis, fragmentary proximal shaft
RR 101	Femur, right, adult
RR 133	Femur, right, adult, lacks proximal half
RR 141	Femur, left, crushed proximal epiphysis, lacks trochanters and distal half of shaft
RR 154	Femur, left, adult, lacks distal half of shaft
RR 161	Femur, left, adult, lacks distal half of shaft
RR 175	Femur, distal epiphysis only
RR 176	Femur, distal epiphysis only
RR 203	Femur, crushed distal epiphysis
RR 237	Femur, left, adult, fragmentary head, separate greater trochanter and intertrochanteric crest
RR 264	Femur, adult, head only
RR 267	Femur left, adult, lacks humeral head and part of distal shaft, broken midshaft, crushed distal epiphysis

Appendix – *continued*

Specimen number	Skeletal material
RR 268	Femur, right, juvenile, crushed, lacks greater tuberosity and distal epiphysis, broken distal to proximal epiphysis
RR 340	Femur, proximal shaft fragment, lacks proximal epiphysis, intertrochanteric fossa and distal half
Tibia	
RR 22	Tibia plateau, left
RR 23	Tibia plateau, crushed
RR 46	Tibia shaft, lacks epiphyses
RR 84	Tibia, right, adult, lacks distal half of shaft and distal epiphysis
RR 134	Tentatively identified, crushed tibial plateau
RR 143	Tibia shaft, crushed distal epiphysis, lacks tibial plateau and tibial tuberosity
RR 148	Tibia, crushed, lacks distal half of shaft and distal epiphysis
RR 301	Tibia, right, crushed shaft, lacks distal epiphysis
Fibula	
RR 96	Fibula, proximal fragment
RR 216	Fibula shaft, crushed proximal epiphysis, lacks distal epiphysis
RR 295	Fibula shaft, crushed distal end, sheared midshaft, lacks proximal end
RR 334	Fibula, lacks distal epiphysis
Patella	
RR 269	Patella
RR 333	Patella
Tarsals	
RR 35	Astragalus, left, lacks medial half
RR 129	Astragalus, left, lacks part of proximal trochlea
RR 213	Astragalus, left
RR 224	Astragalus, right
RR 246	Astragalus, right
RR 290	Astragalus, left
RR 49	Calcaneus?, fragment
RR 164	Calcaneus, right
RR 167	Calcaneus, left
RR 170	Calcaneus, left
RR 290	Calcaneus, left, attached to astragalus
RR 178	Cuboid fragment with astragalar facet
RR 191	Cuboid, left, fragment with plantar process, fragmentary calcaneal and astragalar facets
RR 214	Cuboid, left
RR 229	Cuboid, crushed
RR 240	Cuboid, right, fragment with plantar process, calcaneal facet, incomplete astragalar facet
RR 192	Ectomesocuneiform
Metatarsals	
RR 8	Metatarsal, peripheral
RR 47	Metatarsal, peripheral, crushed epiphysis and plantar tubercle, lacks distal half
RR 76	Metatarsal, central, broken plantar tubercle, lacks distal half of bone
RR 88	Metatarsal, peripheral, with fragmentary proximal epiphysis
RR 105	Metatarsal, central, lacks proximal aspect and shaft
RR 158	Metatarsal, central, crushed, lacks distal part of midshaft and plantar tubercle
RR 199	Metatarsal, peripheral, fragmentary plantar tubercle, dorso-ventrally crushed shaft
RR 280	Metatarsal, lacks proximal half, crushed
RR 291	Metatarsal, central, distal half, lacks proximal half
RR 311	Metatarsal, crushed distal epiphysis, lacks proximal half
RR 139	Metatarsal III, right, proximal cortex damaged, plantar tubercle crushed
RR 225	Metatarsal IV, left, with fragmentary plantar tubercle
Phalanges of the pes	
RR 26	Phalanx, proximal, central
RR 37	Phalanx, proximal, central
RR 118	Phalanx, proximal, central lacks distal epiphysis
RR 132	Phalanx, proximal, central, with sheared shaft
RR 91	Phalanx, peripheral, sheared shaft

Appendix – *continued*

Specimen number	Skeletal material
RR 126	Phalanx, proximal, peripheral, sheared shaft
RR 172	Phalanx, proximal, peripheral, lacks lateral piece of shaft
RR 185	Phalanx, proximal, peripheral, lacks proximal half
RR 200	Phalanx, proximal, peripheral
RR 231	Phalanx, proximal, peripheral
RR 236	Phalanx, proximal, peripheral
RR 275	Phalanx, proximal, peripheral
RR 293	Phalanx, proximal, peripheral, lacks distal end
RR 19	Phalanx, intermediate
RR 34	Phalanx, intermediate
RR 114	Phalanx, intermediate
RR 125	Phalanx, intermediate
RR 181	Phalanx, intermediate
RR 230	Phalanx, intermediate
RR 232	Phalanx, intermediate, lacks distal half
RR 276	Phalanx, intermediate
RR 277	Phalanx, intermediate